Chinese Chemical Letters 34 (2023) 107735

Contents lists available at ScienceDirect

Chinese Chemical Letters

journal homepage: www.elsevier.com/locate/cclet

Recent advances in organic electrosynthesis using heterogeneous catalysts modified electrodes

Li Ma[a,*], Xianang Gao[a], Xin Liu[a], Xiaojun Gu[a], Baoying Li[a], Beibei Mao[b], Zeyuan Sun[a], Wei Gao[a], Xiaofei Jia[c], Jianbin Chen[a,*]

[a] Shandong Provincial Key Laboratory of Molecular Engineering, State Key Laboratory of Biobased Material and Green Papermaking, School of Chemistry and Chemical Engineering, Qilu University of Technology (Shandong Academy of Sciences), Ji'nan, 250353, China
[b] College of Pharmacy, Shandong University of Traditional Chinese Medicine, Ji'nan, 250355, China
[c] Key Laboratory of Optic-electric Sensing and Analytical Chemistry for Life Science, MOE, College of Chemistry and Molecular Engineering, Qingdao University of Science and Technology, Qingdao 266042, China

ARTICLE INFO

Article history:
Received 25 April 2022
Revised 27 July 2022
Accepted 5 August 2022
Available online 10 August 2022

Keywords:
Organic electrosynthesis
Indirect electrosynthesis
Heterogeneous catalysis
Hybrid materials
Electrocatalysis

ABSTRACT

Organic electrosynthesis as an emerging green and advantageous alternative to traditional synthetic methods has achieved remarkable progress in recent years because sustainable electricity can be employed as traceless redox agents. To surmount the over-oxidation/reduction issues of direct electrolysis, mediated or indirect electrochemical processes are attaining remarkable significance and promoting the selectivity of products. Molecular electrocatalysts, benefiting from the easily electronic and steric modulation, suffers from readily degradation issue in most cases. Remarkably, heterogeneous catalysts have drawn more attention due to their high activity, stability, and recyclability. Hence, in this review, the most recent growth of heterogeneous catalysts modified electrodes for organic electrosynthesis were summarized, highlighting structural optimization and electrochemical performance of these materials as well as reaction mechanism. Furthermore, key challenges and future directions in this area were also discussed.

1. Introduction

With increasingly serious energy and environmental issues, reducing pollution at the beginning and developing sustainable chemistry has become particularly urgent. In this regard, organic electrosynthesis has been treated as a green and sustainable alternative to conventional synthetic chemistry. Notably, organic electrosynthesis uses electricity as a clean redox agent to replace the toxic and dangerous chemical redox reagents, realizing electrical-driven chemical reactions. And it is one of the research hotspots in current synthetic chemistry and possesses mild reaction conditions and high atom economy [1–10]. Moreover, chemoselectivity and reaction progress can be precisely controlled by adjusting applied potential, current, and electrode materials [2,11]. Generally speaking, the electrolysis model normally includes direct electrolysis and indirect electrolysis (Fig. 1). Direct electrolysis refers to the direct redox reaction of electroactive species on the surface of the electrode. It mainly depends on the redox potential of the substrate, and maybe suffer from the limited substrate range and difficult compatibility of sensitive groups. Indirect electrolysis provides an alternative strategy, in which an electrocatalyst was used to promote the redox reaction under a mild condition. Compared with direct electrolysis, indirect electrolysis can effectively avoid excessive oxidation/reduction of the substrate, and thus the selectivity of the product is controllable.

Until now, electrocatalysts that have been explored mainly include homogeneous and heterogeneous electrocatalysts [6]. As for homogeneous electrolysis, the reaction was triggered following diffusion of the electrocatalyst to an electrode surface where electron transfer occurs. Several different types of homogeneous electrocatalysts have been developed for organic electrochemical synthesis, such as transition metals-based electrocatalytic C–H functionalization [12,13], cobalt complex-based electrocatalytic organic synthesis [14], *N*-oxyl compounds mediated electrosynthetic reactions [15], halogen-mediated indirect electrosynthesis [16]. Heterogeneous catalysts are the ideal choice to deal with the high cost and environmental issues because of their easy recyclability. Compared with conventional inert electrodes, electrodes modifying with heterogeneous catalysts can provide greatly increased electrochemical active surface area and accelerate the electron transfer between electrode and catalysts, which in turn enhance the utilization efficiency of active sites. Hence, heterogeneous electrocatalysts

* Corresponding authors.
E-mail addresses: li_ma@qlu.edu.cn (L. Ma), jchen@qlu.edu.cn (J. Chen).

https://doi.org/10.1016/j.cclet.2022.08.015
1001-8417/

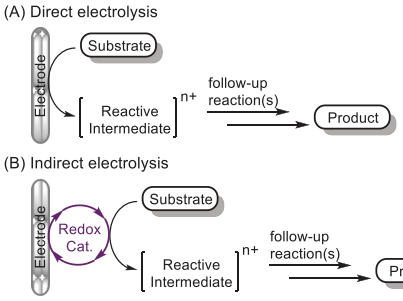

Fig. 1. Two types of electrolysis.

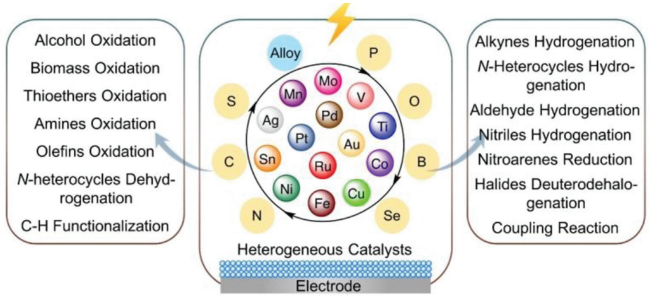

Fig. 2. The representation of heterogeneous catalysts modified electrodes for organic electrosynthesis.

have evoked an immense amount of recent interest due to their high activity, stability, and recyclability. In this review, a series of representative heterogeneous catalysts modified electrodes for organic electrosynthesis were summarized (Fig. 2), highlighting the key features and providing our perspectives on potential directions. We hope this work could promote further development for electrode materials-based versatile organic electrosynthesis.

2. Anodic oxidation reaction

Oxidative reaction is an important tool in synthetic chemistry, enabling the efficient construction of aldehydes, ketones, carboxylic acids, sulfoxides, sulfones, nitriles, *etc.* Traditional method commonly relys on the use of stoichiometric chemical oxidants, such as organic peroxides, hypervalent iodine, and $K_2S_2O_8$, which can often suffer from toxicity, poor functional group compatibility, and substantial amounts of waste. Hence, the development of environmentally benign and user-friendly approach is urgently demanded. To this regard, the adoption of heterogeneous catalysts modified anodes for oxidation reaction is a promising alternative to the traditional oxidation method. The heterogeneous catalysts can be regenerated on anodic oxidation and easily separated from reaction system and reused. It is worth noting that the main by-product is usually the clean energy molecule H_2.

2.1. Electrocatalytic alcohol oxidation

The selective oxidation of alcohols to aldehydes and ketones is one of the most common classes of oxidation reactions in organic chemistry. TEMPO (2,2,6,6-tetramethylpiperidine *N*-oxyl) is a representative homogeneous catalyst for electrochemical oxidation of alcohols and it has achieved widespread application [15,17]. However, the catalytic efficiency is often limited by its slow diffusion rate to the electrode surface and dimerization inactivation. Using a hybrid strategy, several efforts have been made to immobilize the composite of TEMPO and porous materials on electrodes to improve the catalytic efficiency and facilitate recycling [18,19]. For example, Stahl and Das developed that a pyrene–TEMPO con-

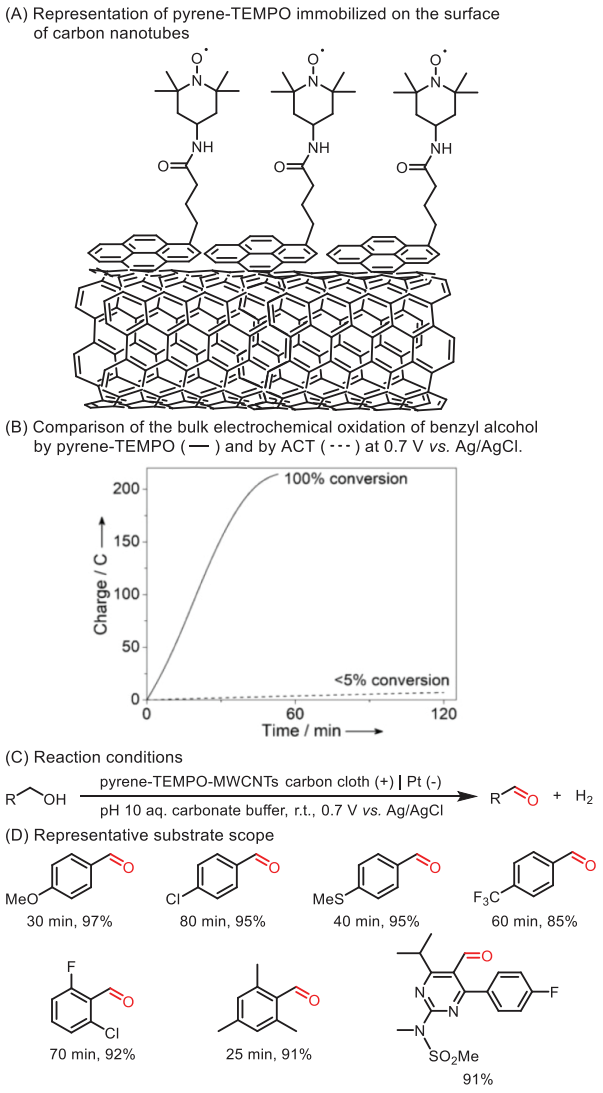

Fig. 3. Pyrene–TEMPO–functionalized electrode electrocatalytic oxidation of alcohols. Reproduced with permission [18]. Copyright 2017, Wiley Publishing Group.

jugate anchored on the electrode which was coated with multi-walled carbon nanotubes (MWCNTs) *via* noncovalent π-π stacking interactions for alcohol oxidation (Fig. 3) [18]. The resulting pyrene-TEMPO-functionalized electrode exhibited outstanding performance in electrocatalytic benzyl alcohol oxidation, far exceeding that of structurally and electronically similar homogenous 4-acetamido–TEMPO (Fig. 3B). This result demonstrated the improved rate of catalyst immobilization on the electrode, which avoided the kinetic loss associated with the transfer of catalyst to and from the electrode surface when a dissolved mediator was employed.

Recently, Wang *et al.* designed CNT/MOL-TEMPO-CO_2^- and CNT/MOL-TEMPO-OPO_3^{2-}, which were prepared by TEMPO-CO_2^- and TEMPO-OPO_3^{2-} *via* ligand exchange with the remaining formates on the MOL SBUs, respectively, to promote selective electrooxidation of alcohols (Fig. 4) [19]. The modified electrodes showed efficient electrocatalytic activity for selective oxidation of primary alcohols in the presence of secondary alcohols (Fig. 4C), which may be attributed to the steric hindrance of the 4-position of TEMPO. In addition, CNT/MOL-TEMPO-OPO_3^{2-} could be reused six times without significant loss of activity.

In the above cases, the immobilization of molecular catalyst (TEMPO) on anodes *via* either noncovalent $\pi-\pi$ stacking interac-

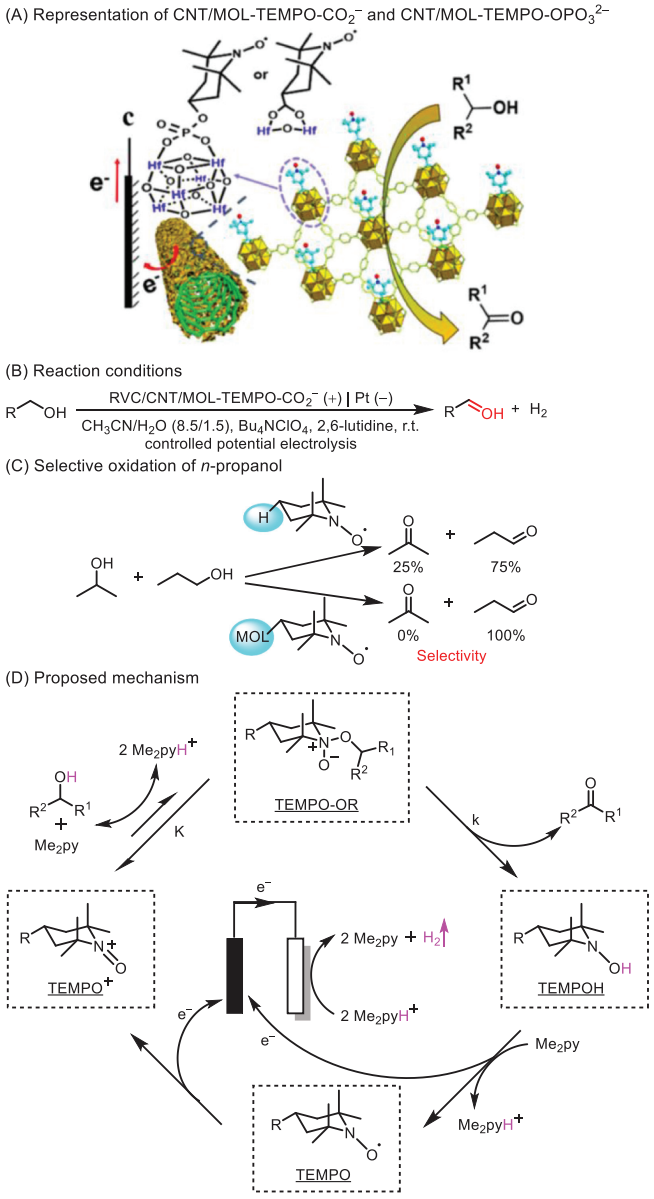

Fig. 4. CNT/MOL-TEMPO modified electrode for electrocatalytic oxidation of alcohols. Reproduced with permission [19]. Copyright 2018, American Chemical Society.

tions or coordination interactions exhibit higher reaction rate and selectivity for electrocatalytic alcohol oxidation than homogenous TEMPO. These results indicate that this method could leave out the step of homogeneous catalyst diffusion to electrode surface and avoid dimerization inactivation of TEMPO. Additionally, with the steric hindrance at 4-position of TEMPO increases, the selectivity also increases. Moreover, this method facilitates the separation of catalysts from the reaction system and the modified anodes can be reused after simple solvent washing. However, long-term instability might be exist by non-covalent immobilization of molecular catalyst.

Apart from these, transition-metal-based catalysts modified electrodes have been reported with appreciable activities for alcohol oxidation [20–22]. Zheng *et al.* reported hierarchical porous nitrogen-doped carbon (NC)@$CuCo_2N_x$ *in-situ* grown on carbon fiber (CF) as a bifunctional electrode for both electrocatalytic oxidation of benzyl alcohol and hydrogen evolution reaction (HER) in alkaline medium [21]. The as-obtained NC@$CuCo_2N_x$/CF anode exhibited remarkable electrocatalytic performance for selective oxidation of benzyl alcohol to benzaldehyde with 96% yield and 95% selectivity. Furthermore, in a two-electrode electrolyzer, paired simultaneous selective electrooxidation of benzyl alcohol and HER was achieved with high conversion and selectivity by employing NC@$CuCo_2N_x$/CF bifunctional electrodes. This was attributed to the hierarchical architecture facilitating to expose more catalytic active sites, enhancing mass transport, and the synergistic effect between CoN and CuN modulating the adsorption energies of key species.

Si *et al.* reported a PdAg bimetallic catalyst *in situ* grown on nickel foam (NF) electrode (PdAg/NF) to promote electro-oxidation of ethylene glycol to glycolic acid [22]. The as-prepared PdAg/NF electrocatalyst exhibited an outstanding performance for highly efficient and selective oxidation of ethylene glycol to glycolic acid with Faradaic efficiency (FE) of 92% under alkaline conditions, much superior to that of Pd/NF and Ag/NF, which could be owing to the synergic effect between Pd and Ag. The density functional theory (DFT) calculations and experimental results indicated that doping of Ag could effectively reduce the adsorption energy of the intermediate which was produced by the Pd-catalyzed dehydrogenation of ethylene glycol (Scheme 1). During the bimetallic synergistic catalysis, $HOCH_2CO^*$ and OH^* were adsorbed on the Pd and Ag, respectively, and produced glycolic acid without breaking the C-C bond, thus significantly improving the ethylene glycol oxidation activity and glycolic acid selectivity.

As modifiers of anodes, inorganic heterogeneous catalysts are also proved to be the critical catalytic centers for electrocatalytic alcohol oxidation. Due to the porous structures, the reactants can be facilitated to contact with the catalytic sites as well as enhanc-

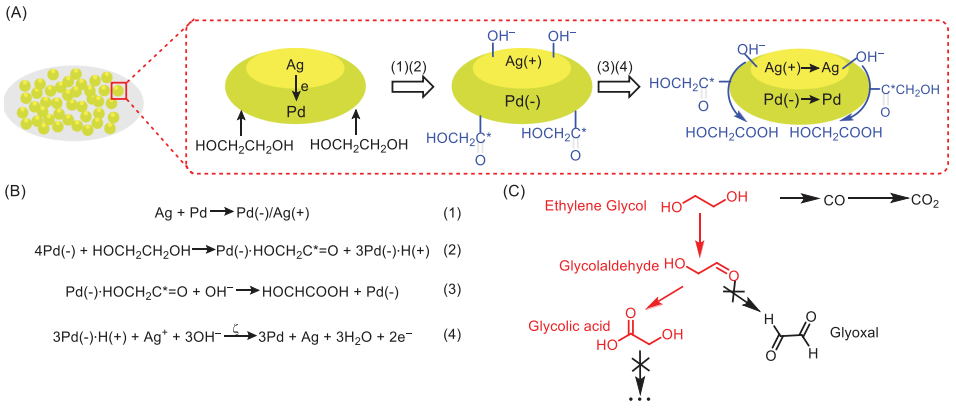

Scheme 1. Schematic illustration of the proposed synergetic catalytic effect between Pd and Ag. (A,B) A probable mechanism of the synergetic catalytic effect for ethylene glycol oxidation on the PdAg/NF catalyst. (C) General pathway of ethylene glycol oxidation (the red is proposed to be the dominant pathway in this work).

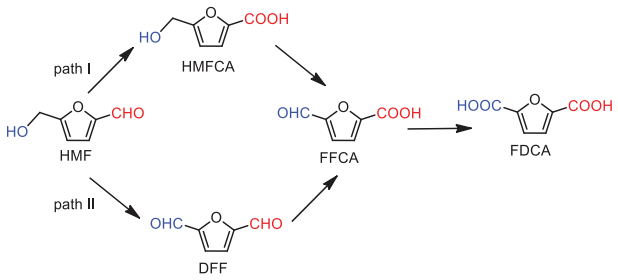

Scheme 2. Two possible pathways of HMF oxidation to FDCA.

ing mass transport. By tuning the adsorption energies of metals to key intermediate species, the oxidation activity and selectivity of the reaction are regulated.

2.2. Electrocatalytic biomass oxidation

Catalytic synthesis of value-added chemicals from renewable biomass has received great attention in recent years. The advance of biomass oxidation has been well summarized in several previous reviews [23–26], thus this section will outlines the development of electrocatalytic biomass oxidation, aiming to draw community attention to this emerging field. As early as 1991, Grabowski *et al.* pioneered in this area and firstly reported $Ni(OH)_2$/NiOOH-covered Ni mesh as anode electrocatalytic oxidation of 5-hydroxymethylfurfural (HMF) to 2,5-furandicarboxylic acid (FDCA) in an alkaline electrolyte (1.0 mol/L NaOH), giving 71% yield because of decomposition of HMF in strong alkaline solutions [27]. Since then, various heterogeneous catalysts modified electrodes for the electrochemical oxidation of HMF have been reported, and the oxidation pathway relates to the catalyst type and oxidation potential. For example, Chadderdon *et al.* reported that carbon-black-supported Au and Pd bimetallic nanoparticles (NPs) were painted onto the carbon cloth (CC) anode for electrocatalytic oxidation of HMF to FDCA (Scheme 2) [28]. The experimental results revealed that the applied electrode potential and catalyst surface composition played a pivotal role in competitive oxidation between aldehyde and alcohol groups of HMF. Au/C electrode favored the oxidation of aldehyde group to obtain 5-hydroxymethyl-2-furancarboxylic acid (HMFCA), but required higher electrode potentials to further oxidize alcohol group to form FDCA. And Pd/C electrode followed two competitive routes to oxidize HMF to FDCA, but needed high potentials to promote this process. Interestingly, the Pd-Au bimetal modified electrode exhibited much higher catalytic performance at lower potentials than those of Au/C and Pd/C electrodes. Additionally, the bimetallic catalyst with 1:2 Pd/Au molar ratio showed the optimal electrochemical performance with 83% yield of FDCA at the potential of 0.9 V *vs.* RHE after 1 h.

Park *et al.* proposed tailorable 3D hybrid multilayer electrodes for electrochemical oxidation of HMF (Fig. 5) [29]. The modified electrodes were prepared by Au, Pd, or their alloy NPs with nano-sized graphene oxide (nGO) through layer-by-layer (LbL) assembly onto indium tinoxide (ITO) substrates. This approach takes advantage of precise regulation of the internal architecture of the LbL-assembled multilayer (including the thickness and position of Au and Pd NPs) to study the relationship between the nanoarchitecture of the modified electrodes and electrocatalytic activity. Interestingly, even the composition of NPs is the same, the Pd_7/Au_7 electrode with Au NPs located at the outer layer exhibited a higher yield of FDCA than that of the Au_7/Pd_7 electrode, which was attributed to the enhanced mass transfer into the inner-layer Pd NPs. In addition, the optimized LbL-assembled two-electrode system of Pd_7/Au_7 || $(AuPd)_7$ displayed the best full-cell electrocatalytic activity for both HMF oxidation at the anode and HER at the cathode.

In a subsequent study, non-precious metal-based catalysts modified electrodes have been developed to replace noble metal-based electrodes for electrocatalytic oxidation of HMF to FDCA. For instance, transition metal phosphides [30–32], sulphides [33], borides [34–36], and nitrides [37,38] have been reported with promising electrocatalytic HMF oxidation performances and can be used several successive electrolysis cycles without obvious loss in activity. As an example, Zhang *et al.* developed NiB_x as a catalyst *in-situ* grown on NF electrode for electrochemical oxidation of HMF using H_2O as an oxygen source (Fig. 6) [36]. The as-prepared NiB_x@NF anode exhibited high conversion of HMF to FDCA and excellent FE with the value of 99.8% and 99.5%, respectively. A plausible mechanism was proposed as well. At the NiB_x@NF anode, Ni^{3+} with a newly bonded OH^- originating from H_2O was formed *via* the electrooxidation of Ni^{2+}, and followed by reacting with HMF, DFF and/or HMFCA to obtain FDCA, accompanied by the regeneration of Ni^{2+}. Additionally, in a paired electrosynthesis system, NiB_x@NF as bifunctional electrodes could simultaneously enable

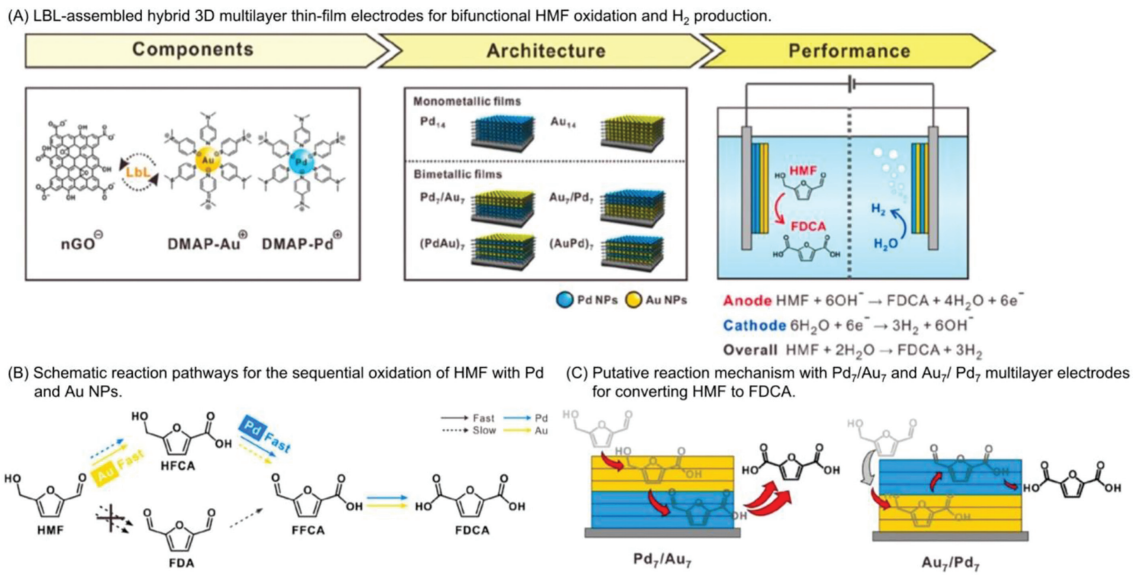

Fig. 5. Au and Pd alloy modified electrode for electrocatalytic oxidation of HMF. Reproduced with permission [29]. Copyright 2020, American Chemical Society.

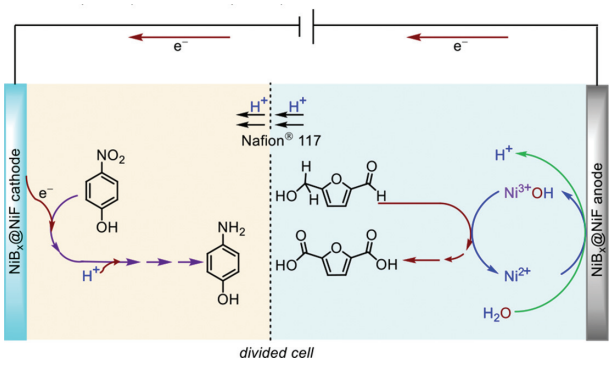

Fig. 6. NiB_x modified electrode for electrocatalytic oxidation of HMF.

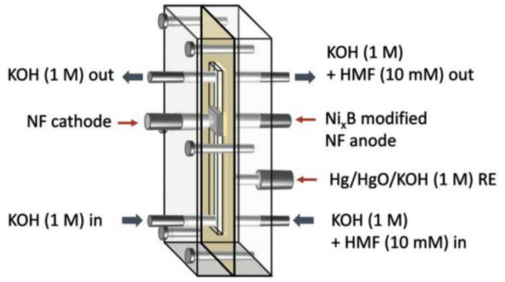

Fig. 7. The electrochemical flow reactor for continuous HMF electrochemical oxidation. Reproduced with permission [34]. Copyright 2018, Wiley Publishing Group.

the oxygenation of HMF and the hydrogenation of *p*-nitrophenol with conversion efficiency and FE above 99%.

Recently, Barwe *et al.* achieved a high-surface-area Ni_xB modified NF anode to electrocatalytic oxidation of HMF to FDCA in an electrochemical flow-through reactor (Fig. 7) [34], which could enable the efficient and safe scale-up of electrochemical processes for industrial applications.

In recent years, metal-based oxides [39–52], hydroxides [53–56], and oxyhydroxides [57,58] exhibit fascinating electrocatalytic HMF oxidation activities. For example, Gao *et al.* investigated the performance of different morphologies of $Ni_xCo_{3-x}O_4$ nanostructure for electrocatalytic oxidation of HMF to FDCA [39]. Zhang *et al.* employed Co_9S_8–Ni_3S_2@N,S,O-tri-doped carbon heterostructures catalyst to realize efficient HMF conversion to FDCA [59]. Zhou *et al.* disclosed that the abundant surface defects of CoNW/NF could facilitate the electrochemical oxidation of HMF into FDCA [41]. Huang *et al.* achieved rich oxygen vacancies *via* Se doping in CoO and demonstrated outstanding electrocatalytic HMF oxidation performance due to the increased electrochemical surface area as well as reduced charge transfer resistance [43]. Liu *et al.* discovered bimetallic NiFe layered double hydroxide (LDH) nanosheets *in-situ* grown on carbon fiber paper (CFP) could promote electrocatalytic oxidation of HMF to FDCA, owing to the thin nanosheets structure feature promoting the exposure of more catalytic active sites [53].

Mechanistically, it is widely accepted that Ni and Co species played critical roles in Ni and Co-based electrocatalysts. For the Ni-based catalysts, Choi *et al.* achieved NiO NPs modified carbon paper (CP) electrode for electrochemical oxidation of HMF, and demonstrated that the $Ni(OH)_2$ intermediate was first formed on the surface of NiO in the alkaline medium, then it was easily oxidized into Ni(III)-OOH during HMF oxidation. Adsorbed alcohol could be oxidized when Ni(III)-OOH returns to $Ni(OH)_2$, and the HMF oxidation occurred *via* the DFF pathway [44]. Zhou *et al.* proposed that the deposition of Pt NPs into $Ni(OH)_2$ modified electrode could promote electrocatalytic oxidation of HMF to FDCA [56]. The as-synthesized Pt/$Ni(OH)_2$ exhibited highly efficient electrocatalytic performance for HMF oxidation, 8.2 times enhancement than that of $Ni(OH)_2$. This study demonstrated that the doping of Pt could optimize the redox properties of $Ni(OH)_2$, resulting in the accelerated formation of Ni(OH)O, which was confirmed by operando methods. On the other hand, it was also proved that Pt could serve as the adsorption site of HMF, reducing the adsorption energy of HMF with optimized adsorption behavior. Recently, Zhou *et al.* explored the activity origin of Ni_3N *via* operando X-ray absorption spectroscopy (XAS), *quasi in situ* X-ray photoelectron spectroscopy (XPS), *in situ* Raman, and operando electrochemical impedance spectroscopy (EIS), and proved that $Ni^{2+\delta}N(OH)_{ads}$ generated by the adsorbed hydroxyl group was the activity origin [60]. Taitt *et al.* systematically investigated and compared three different MOOH anodes (M = Ni, Co, Fe) for HMF electrooxidation in a 0.1 mol/L KOH solution [57]. The NiOOH anode exhibited the best catalytic performance with 96% FDCA yield at 1.47 V *vs.* RHE, whereas CoOOH and FeOOH anodes only achieved FDCA yield of 35% (at 1.56 V *vs.* RHE) and <5% (at 1.71 V *vs.* RHE), respectively. Although the CoOOH anode could initiate HMF oxidation at a less positive potential than NiOOH anode benefiting from the $Co(OH)_2$/CoOOH couple conversion occurred at a lower redox potential, the rate of $Co(OH)_2$/CoOOH-mediated HMF oxidation was not fast enough to produce sufficient current density for constant potential HMF oxidation. Recently, Kornienko and Heidary studied the NiOOH catalyst using operando surface-enhanced Raman spectroscopic, demonstrating that in 10 mmol/L KOH solution, the reaction proceeded *via* the DFF pathway, whereas in 1 mol/L KOH solution, it followed the HMFCA pathway [58].

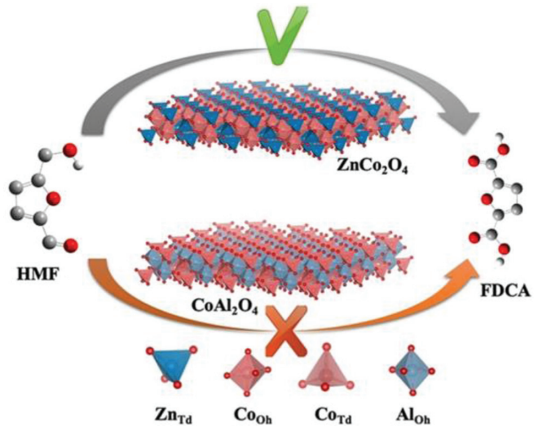

Fig. 8. $Co^{3+}{}_{Oh}$ plays a decisive role in HMF oxidation. Copied with permission [61]. Copyright 2020, Wiley Publishing Group.

For the Co-based catalysts, Lu *et al.* investigated Co-based spinel oxides as working electrodes for electrochemical oxidation of HMF to FDCA [61]. By the substitution of the tetrahedral site ($Co^{2+}{}_{Td}$) and octahedral site ($Co^{3+}{}_{Oh}$) in Co_3O_4 with Zn^{2+} and Al^{3+}, respectively (Fig. 8), the authors confirmed that $Co^{3+}{}_{Oh}$ was the optimal geometrical configuration for the oxidation of HMF and $Co^{2+}{}_{Td}$ could provide chemical adsorption sites. Based on these, replacing $Co^{2+}{}_{Td}$ with Cu^{2+} to enhance the exposure degree of $Co^{3+}{}_{Oh}$ and boost acidic adsorption, the obtained $CuCo_2O_4$ exhibited a record performance among Co-based catalysts and four times higher than that of Co_3O_4. Similarly, based on the geometrical configuration of the metal oxides, Lu *et al.* prepared a 3D hierarchically nanostructured NiO-Co_3O_4 *in-situ* grown on the NF electrode for electrocatalytic oxidation of HMF [62]. The crystal structures of Co_3O_4 and NiO are spinel and face-center cube, respectively, thus the atom permutation cannot be one-to-one correspondence at the interface, providing abundant defects and vacancies. And these vacan-

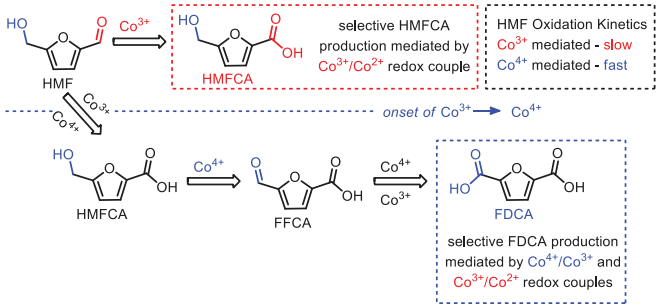

Fig. 9. Mechanistic illustration of potential-dependent oxidation of HMF to produce HMFCA and FDCA as mediated by electrogenerated Co^{3+} and Co^{4+} species

cies played a decisive role in electrocatalytic HMF oxidation, bringing a high yield of FDCA (98%) and FE (96%).

In addition, Deng *et al.* firstly reported the oxidation of HMF could be selectively regulated by changing the oxidation state of the Co-based electrocatalyst electrodeposited on CC electrode (Fig. 9) [63]. Employing CoO_xH_y as the model electrocatalyst, it was found that Co^{3+} formed at low potential acted as a sluggish oxidant for the oxidation of formyl group exclusively to carboxylate, while Co^{4+} generated at high potential was necessary for the initial and spontaneous oxidation of hydroxyl group in HMF with significantly faster kinetics. As a result, the oxidation products of HMFCA and FDCA could be conveniently tuned by adjusting the applied potential.

Porous framework materials, such as metal-organic frameworks (MOFs) [64] and covalent-organic frameworks (COFs) [65,66], always have periodic crystal structures with high surface area, porous channels, and tunable structure, making them ideal as promising candidates for catalysis [67–76]. Cai *et al.* firstly reported Ni-based two-dimensional (2D) MOF nanosheets grown on NF electrode for electrochemical oxidation of HMF (Fig. 10A) [77]. The as-prepared Co-doped 2D MOFs NiCoBDC/NF exhibited a superior activity in contrast with NiBDC/NF, NiFeBDC/NF, and NiMnBDC/NF, obtaining 99% yield of FDCA and 78.8% FE in a pH 13 medium at 1.55 V *vs.* RHE. And it remained 95% yield and 75% FE within four successive electrolysis cycles. Later, Bai *et al.* investigated MOF nanoarray modified NF electrode by *in-situ* hydrothermally deposited for electrochemical oxidation of HMF (Fig. 10B) [78]. The as-prepared ternary CoNiFe-MOFs/NF electrode exhibited highly active electrooxidation of HMF to FDCA with FE of 100% and yield of 99.76% in a 1.0 mol/L KOH solution. Furthermore, the modified electrode could be reused for 15 consecutive cycles without significant loss in activity. In 2020, Cai *et al.* reported Ni(II)-doped COF film immobilized on FTO electrode for electrochemical oxidation of HMF in alkaline solution (Fig. 10C) [79]. The as-prepared TpBpy-Ni@FTO gave a 96% conversion of HMF and 58% yield of FDCA.

Apart from these, Wu *et al.* firstly described metal chalcogenides (MC) modified CP electrodes for the electrochemical oxidation of furfural to 5-hydroxy-2(5*H*)-furanone (HFO) using H_2O as the oxygen source (Fig. 11) [80]. As a comparison, the as-prepared CuS/CP anode exhibited the best performance with 70.2% conversion of furfural and 83.6% selectivity of HFO than the other prepared MC/CP electrodes (*i.e.*, ZnS/CP, CdS/CP, PbS/CP, WS_2/CP and MoS_2/CP). Furthermore, CuS/CP anode provided excellent long-term stability to maintain the FE and selectivity of HFO with 77.8% and 85.3%, respectively, within a reaction time of 24 h. Mechanism studies indicated that HFO was achieved by a multi-step reaction depicted in Fig. 11B, including the C-C bond cleavage of furfural, succeeding by ring-opening and oxidation, as well as intramolecular isomerization.

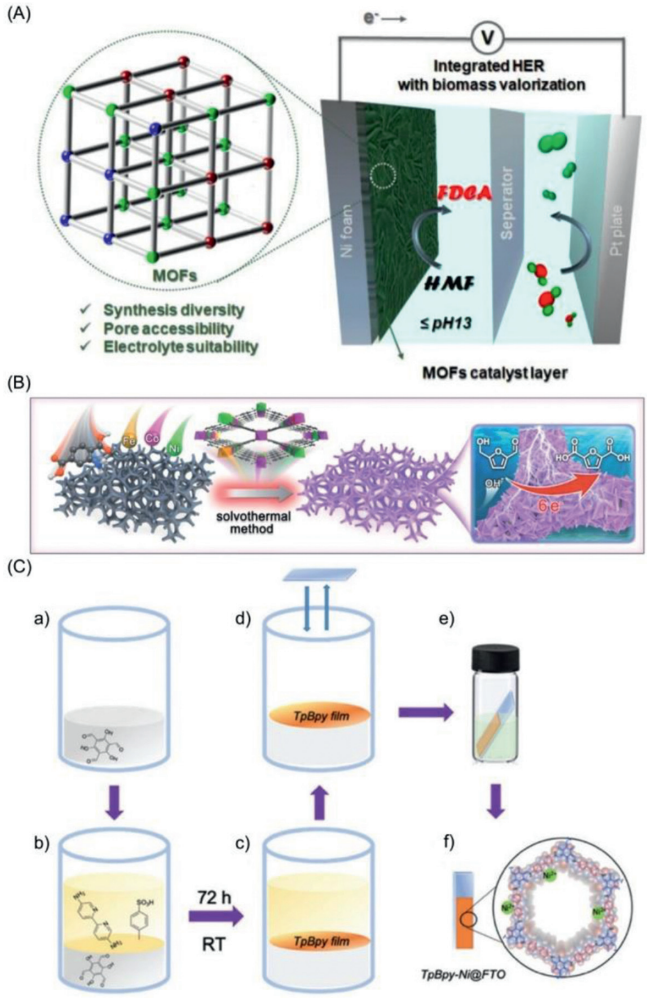

Fig. 10. (A) 2D MOFs catalyst for electrocatalytic HMF oxidation. Copied with permission [77]. Copyright 2020, Royal Society of Chemistry. (B) Schematic representation for the fabrication of trimetallic MOF arrays on NF and the application of electrocatalytic HMF oxidation. Copied with permission [78]. Copyright 2021, Royal Society of Chemistry. (C) Schematic illustration of the preparation of TpBpy-Ni@FTO. Copied with permission [79]. Copyright 2020, Royal Society of Chemistry.

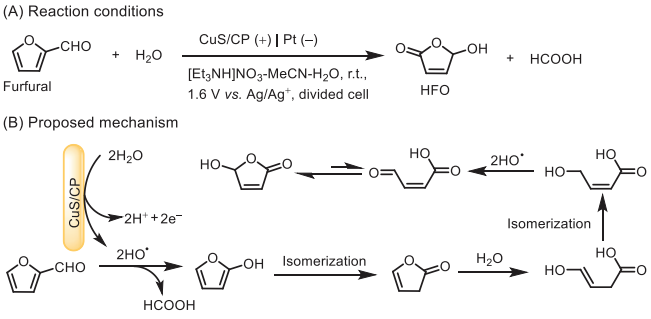

Fig. 11. CuS modified electrode for electrocatalytic furfural oxidation.

Additionally, Zhang *et al.* explored metal phosphides (Ni_2P or Cu_3P) *in situ* grown on carbon fiber cloth (CFC) electrode *via* a facile vapor-phase hydrothermal route for electrocatalytic oxidation of furfural [81]. Compared to the Cu_3P/CFC, the as-obtained Ni_2P/CFC exhibited more superior activity for the furfural oxidation with almost 100% selectivity of furoic acid product and over 90% FE in alkaline electrolyte. These results might be mainly at-

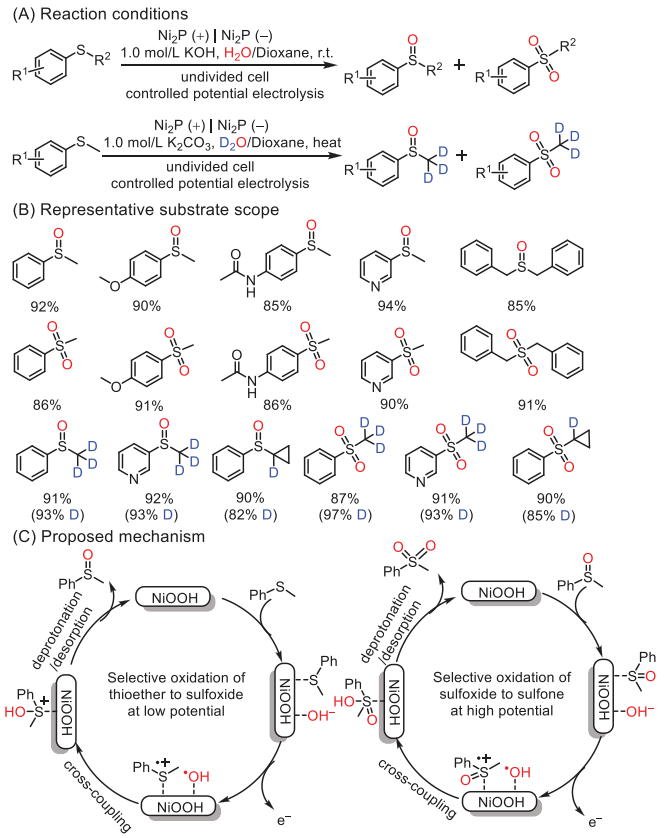

Fig. 12. Ni_2P hollow nanocubes modified electrode for selective thioether electrooxidation.

tributed to the formation of high valence state Ni species, such as oxides/hydroxides and oxyhydroxides.

As for the catalysts in indirect electrolysis, transition-metal-based heterogeneous materials are proved to be critical points to improve the electrochemical performance for biomass oxidation. The material nanostructures, metal catalytic sites, surrounding chemical environment, and morphologies all benefit the development of advanced heterogeneous electrocatalysts with high performance.

2.3. Electrocatalytic thioethers oxidation

Sulfoxide and sulfone skeletons are invaluable structural components in pharmaceuticals and functional materials [82,83]. Traditional procedure to construct this skeleton mainly relied on selective oxidation of thioether using homogeneous catalysts with O_2 or H_2O_2 as the main oxygen sources [84,85]. Obviously, the cost, safety and product purification are the disadvantages. Recently, the electrooxidation of thioether has been developed. However, it suffers from limited noble metal electrodes, expensive electrolytes and O_2 [86,87]. To solve this issue, Han *et al.* investigated nickel phosphide (Ni_2P) hollow nanocubes modified NF electrode for membrane-free selective thioether electrooxidation with H_2O as the oxygen source (Fig. 12) [88]. By adjusting the potential, the controllable synthesis of sulfoxides and sulfones could be achieved with high yields and selectivity. The surface *in-situ* reconstruction of Ni_2P to NiOOH played a pivotal role in assisting the formation of Ni^{II}/Ni^{III} redox couple. The reaction was initiated by the oxidation of thioethers which was adsorbed on the Ni site of NiOOH, generating the radical cation. And •OH was formed at the same time *via* water electrolysis, followed by the radical cross-coupling and deprotonation to accomplish the sulfoxides. Sulfones could be obtained at a higher oxidation potential through a similar process with sulfoxides as the substrates. As a comparison, bare NF, Pt and CFP anodes were inert in the low potential system, whereas Ni_2P nanosheets and Ni_2P nanoparticles modified anodes delivered low yields of sulfoxides. These results also demonstrated that high valance Ni species were the actual active centers, and the morphologies of Ni_2P also affected catalytic performance. The excellent catalytic performance of Ni_2P hollow nanocubes might be due to its higher surface area and exposure of more catalytic active sites than Ni_2P nanosheets and Ni_2P nanoparticles. In addition, the Ni_2P hollow nanocubes modified anode could be recycled six times without a significant decrease in catalytic activity. And this method displayed broad functional group compatibility and easily synthesized deuterated sulfoxides and sulfones.

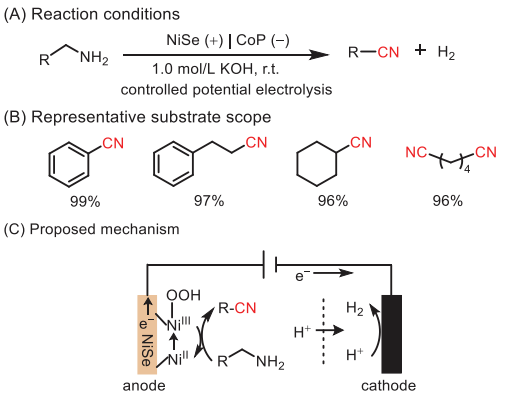

Fig. 13. NiSe nanorod modified electrode for primary amines electrooxidation.

2.4. Electrocatalytic primary amines oxidation

Nitriles are useful intermediates for the synthesis of pharmaceuticals, agrochemicals, and fine chemicals [89–91]. Selective oxidation of primary amines to nitriles could avoid the use of HCN or metal cyanides [92]. Unfortunately, most of the reported methods usually require high temperature and/or high O_2 pressure with the presence of additives for oxidation [93–95]. Hence, replacing thermocatalysis with electrocatalysis might be an effective solution. Huang *et al.* developed a NiSe nanorod anode prepared by direct selenization of commercially NF to promote oxidant-free electrooxidation of primary amines to the corresponding nitriles at room temperature (Fig. 13) [96]. At the NiSe nanorod anode, the surface Ni^{II} was first oxidized to form $Ni^{III}OOH$ in alkaline solution, which then oxidized primary amines into nitriles, along with conversing $Ni^{III}OOH$ into Ni^{II} (Fig. 13C). A wide range of structurally diverse nitriles were prepared in excellent yields. The non-water-soluble feature of nitriles could easily escape from the aqueous electrolyte/electrode interface, avoiding catalyst deactivation. Moreover, NiSe nanorod anode remained highly active within six runs and favored the continuous gram-scale nitrile production with industrial practicability. Notably, replacing sluggish oxygen evolution reaction with electrooxidation of thermodynamically more favorable primary amines in water splitting system, the cell voltage was significantly reduced relative to that of overall water splitting. Similarly, Mondal *et al.* declared a crystalline intermetallic nickel silicide catalyst (Ni_2Si NPs) prepared by a simple one-pot colloidal approach, aiming to produce high-value oxidation and reduction products (nitriles and H_2, respectively) [97]. The active phase $Ni^{III}O_xH_y$ was formed by accompanying the corrosion of Si to silicate under alkaline condition. The Dissolution of Si might result in more porous $Ni^{III}O_xH_y$ phase with a distorted layered structure and facilitate electrolyte penetration. Furthermore, the activated form of Ni_2Si exhibited highly efficient electrocatalytic oxidative dehy-

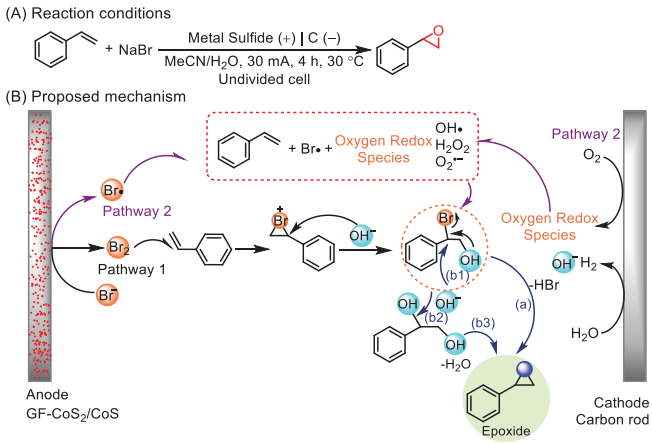

Fig. 14. GF-CoS_2/CoS anode for electrocatalytic epoxidation.

drogenation of primary amines with high selectivity and a wide range of substrates.

2.5. Electrocatalytic olefins oxidation

Epoxides as one of important class of intermediates are widely used in the manufacture of many chemical products. Typically, epoxides are synthesized *via* olefin epoxidation in which the use of hazardous reagents or the generation of stoichiometric side products present challenges for separation and waste streams. In this regard, electrosynthesis has provided an eco-friendly approach to achieve the selective oxidation due to the toxic reagents can be replaced with electricity.

Previous works demonstrated that NaBr was used as a mediator for electrocatalytic epoxidation and obtained good selectivity of olefins [98–100]. However, the used Pt electrode suffers from the corrosion by Br^-, while carbon-based electrodes showed particularly low catalytic activity towards NaBr mediator. To address this issue, Zhang *et al.* proposed using GF-CoS_2/CoS heterostructures anchored on graphite felt (GF-CoS_2/CoS) to trigger Br^-/Br_2 redox mediator (Fig. 14) [101]. The experimental results showed GF-CoS_2/CoS anode is superior to the Pt electrode in catalyzing Br^-/Br_2 redox mediator. Under the optimized reaction conditions, the epoxidation of styrene with 97% yield was obtained using GF-CoS_2/CoS anode at 30 mA/cm^2. Importantly, the applied voltage on the GF-CoS_2/CoS-based electrode system was reduced to 4-5 V compared to 7.8–9.3 V on the Pt-based electrode system, saving half of the energy.

In order to facilitate the separation of catalyst from the reaction system and avoid the use of additional reagents, Jin *et al.* demonstrated a sustainable and green route to epoxidation reactions. They used Mn_3O_4 nanoparticles modified carbon paper as the anode and H_2O as safe oxygen atom source (Fig. 15) [102]. The experiment results indicated Mn^{IV}-oxo species played a pivotal role in this electrochemical oxidation and isotopic studies revealed H_2O as the sole oxygen atom source. In addition, the modified electrodes exhibited efficient catalytic epoxidation of cyclooctene with FE above 30% at the anode and coproduction of H_2 with FE above 94% at the cathode. Unfortunately, the FE and yields of electrocatalytic olefins oxidation are not high enough, and much work need to be further explored.

2.6. Electrochemical N-heterocycles dehydrogenation

The catalytic acceptorless dehydrogenation of *N*-heterocycles is a dominant strategy to access quinoline and indole rings, which are frequently encountered in pharmaceuticals and bioactive

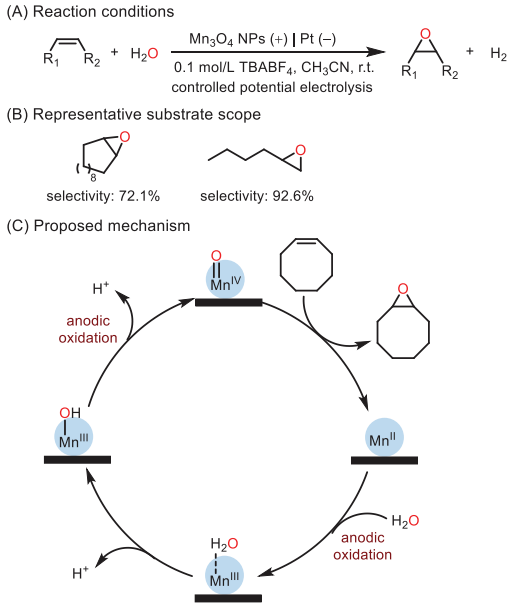

Fig. 15. Mn_3O_4 NPs modified electrode for epoxidation of olefins.

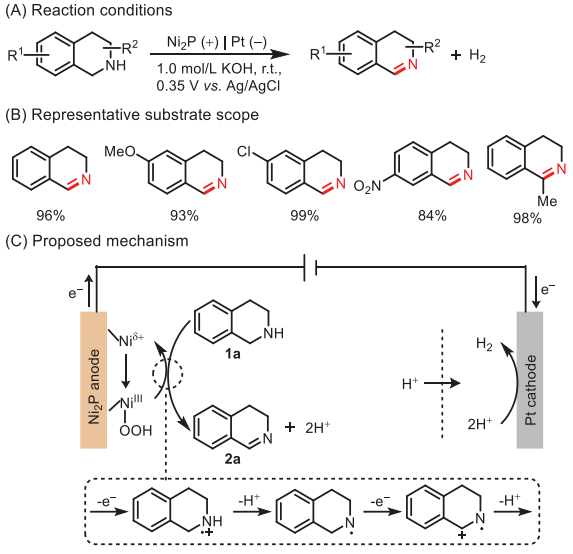

Fig. 16. Ni_2P modified electrode for electrochemical semi-dehydrogenation of tetrahydroisoquinolines.

molecules. Traditional dehydrogenation needs oxidants or sacrificial hydrogen acceptors, which often generate undesirable byproducts such as toxic metal salts [103,104]. At present, electrochemistry has offered an efficient way to achieve acceptorless dehydrogenation with H_2 production. In addition, replacing homogeneous catalysts with heterogeneous catalysts could avoid the tedious separation step and the contamination of the products. In 2019, Huang *et al.* explored the use of a Ni_2P bifunctional electrode to promote selective semi-dehydrogenation of tetrahydroisoquinolines (THIQs) (Fig. 16) [105]. Preparation of the modified electrode by immersing the nickel foam into $Ni(NO_3)_2 \cdot 6H_2O$ aqueous solution, followed by annealing and phosphidation. The Ni_2P nanosheet electrode exhibited high activity at controllable electrooxidation from THIQs to dihydroisoquinolines (DHIQs), as well as the production of H_2 at the same time. At the anode, Ni^{III}-OOH was first formed and then it oxidized **1a** to **2a**. A wide range of structurally diverse DHIQs were obtained in good yields and excellent selectivity. Remarkably, the Ni_2P electrode could be recycled up to 6 times without significant

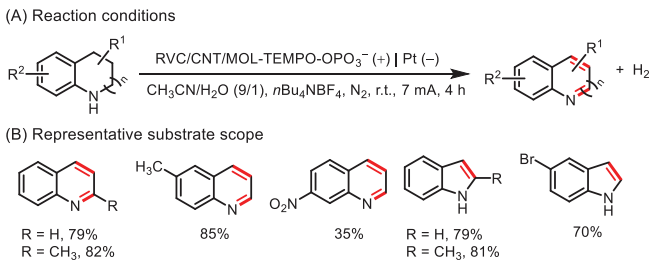

Fig. 17. CNT/MOL-TEMPO-OPO_3^{2-} modified electrode for electrocatalytic dehydrogenation of *N*-heterocycles.

loss in electrocatalytic activity and maintained the nanosheet arrays morphology. Then, Li *et al.* prepared a Ni-Mo catalyst as both the cathode and anode to achieve hydrogenation and dehydrogenation of *N*-heterocycles using water as the H source [106]. Mo atom with superior hydrogen adsorption property could accelerate the generation of active H* species, promoting hydrogenation of the quinoxaline. And Ni component could be electrooxidized to NiOOH leading to the formation of Ni^{II}/Ni^{III} redox couple, which facilitated the oxidative dehydrogenation of hydrogenated quinoxaline. Subsequently, Wang *et al.* reported Co_3O_4@NiO bifunctional electrodes could enable electrocatalytic semi-dehydrogenation of THIQs and simultaneous electroreduction of nitrate [107]. The modified electrode was prepared by coating Co_3O_4@NiO HNTs on CP electrode, in which Co_3O_4@NiO HNTs were prepared by using adopting Co-aspartic acid nanowires (Co-Asp NWs) as precursors *via* the cation-exchange reaction with Ni^{2+} and followed by annealing. The supported Co_3O_4@NiO HNTs catalyst displayed excellent activity and selectivity for both anodic THIQs semi-dehydrogenation to DHIQs and cathode nitrate electroreduction to ammonia. And Ni^{III}-OOH and NO were the key intermediates for both reactions, respectively. In addition, Yang *et al.* reported the CNT/MOL-TEMPO-OPO_3^{2-} electrode could promote dehydrogenation of *N*-heterocycles (Fig. 17) [108]. A range of quinoline or indole derivatives were obtained in moderate to good yields and the hybrid catalyst could be reused three times without loss of activity.

2.7. Electrocatalytic C–H functionalization

C–H functionalization is of great interest to upgrade the primary raw materials [109,110]. However, the stubborn C–H bonds usually make their activation quite challenging, and harsh conditions such as high temperatures, toxic oxidants, and noble-metal catalysts have to be required to achieve acceptable conversions [111–113]. To address this issue, electrosynthesis instead of traditional thermocatalysis might be an effective solution. Li *et al.* reported W_2C/N_xC catalysts modified CC anode for alkoxylation of benzylic C–H bonds (Fig. 18) [114]. $W_2C/N_{3.0}C$ electrode as the best-in-class anode exhibited excellent selectivity and good to high conversions for electrochemical alkoxylation of various aromatic C–H bonds, which was superior to the commercial electrodes (boron-doped diamond, reticulated vitreous carbon, and lead oxide). Moreover, replacing $W_2C/N_{3.0}C$ catalysts with W_2C catalyst, NC sample, or a mechanical mixture of the two components obtained much lower conversions under the same conditions. This strongly implied a synergistic effect between W_2C and $N_{3.0}C$ components. In addition, without an obvious decrease in FE was observed after four cycles, indicating the great electrochemical stability of $W_2C/N_{3.0}C$ anode. The theoretical calculations and experimental results revealed that regulating the electron density of W_2C nanocrystals *via* the construction of Schottky heterojunctions with N-doped carbon could enhance the superior adsorption of benzylic C–H bonds on the W_2C surface, promoting the activation of C–H bonds, which was the rate dominating step.

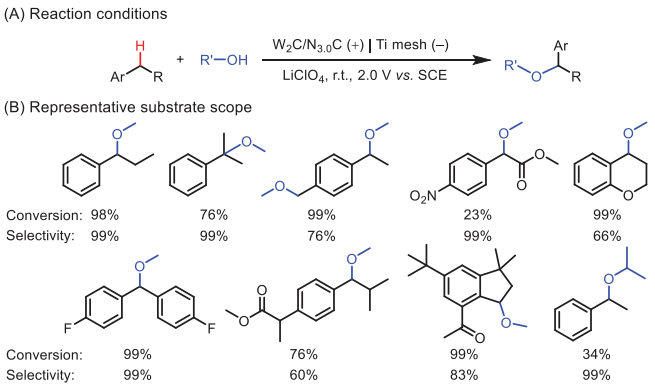

Fig. 18. $W_2C/N_{3.0}C$ modified electrode for alkoxylation of benzylic C–H bonds.

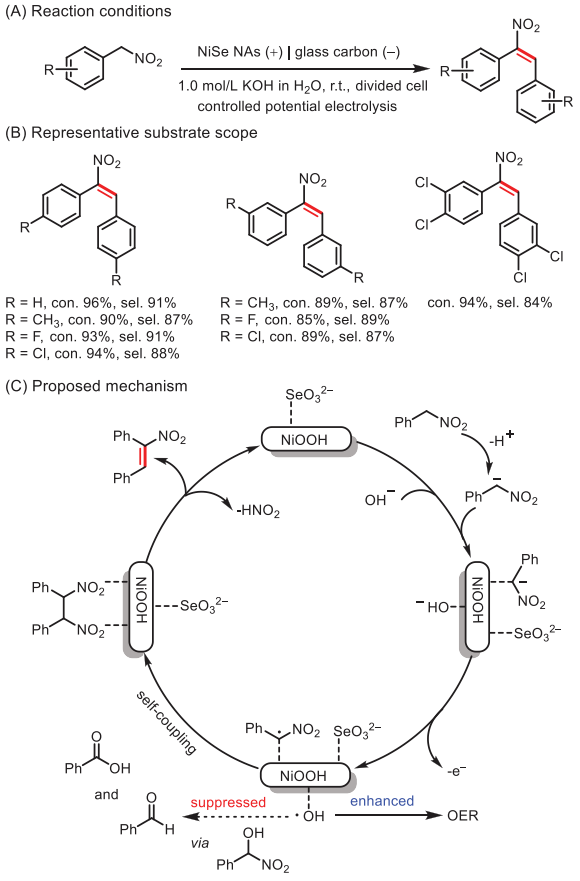

Fig. 19. NiSe NAs modified electrode for electrochemical self-coupling reaction.

Recently, in another work by the Zhang's group, NiSe nanorod arrays (NAs) *in-situ* grown on NF electrode was employed to promote the electrooxidation of α-nitrotoluene to *E*-nitroethene (Fig. 19) [115]. The *in-situ* formed NiOOH surface layer, surface adsorbed SeO_x^{2-} through Se leaching-oxidation during electrooxidation, as well as the preferential adsorption of intermediate with two $-NO_2$ groups on NiOOH played a crucial role for NiSe NAs anode to highly efficient electrooxidize α-nitrotoluene to *E*-nitroethene with 99% selectivity, 89% FE, and the reaction rate of 0.25 mmol cm^{-2} h^{-1}. A plausible mechanism was proposed as well (Fig. 19C). The α-carbon radical was generated by the oxidation of α-carbon anion at the anode, followed by self-coupling to form the intermediate with two -NO_2 groups, and then a HNO_2 molecule was eliminated to obtain the desired products. This protocol displayed broad functional group compatibility and various *E*-nitroalkenes were ob-

tained with good to high selectivity and high yields. Furthermore, the reaction could also be easily achieved at the gram scale with high selectivity and conversion yield.

3. Cathodic reduction reaction

In constrast to indirect electrooxidation reations, the indirect electroreduction remains relatively underexplored. Recently, electroreduction has received increasing attention due to its tunable reducing potential and good scalability, while avoiding the use of stoichiometric reductants (reducing metals, organic compounds, *etc.*) in traditional reduction methods. Currently, a variety of inorganic heterogeneous catalysts (transition metal phosphides, sulfides, alloy, *etc.*) have been demonstrated as efficient reductants for hydrogenation reaction, deuterodehalogenation reaction and coupling reaction.

3.1. Electrocatalytic hydrogenation of alkynes

Selective hydrogenation of alkynes to alkenes is of great importance in chemical synthesis. Unfortunately, it usually requires harsh conditions, such as high temperature and/or high H_2 pressure. To address these issues, replacing traditional thermocatalysis with electrocatalysis and combinating with electroreducing water where hydrogen is generated *in situ*, might be an effective solution. Zhang *et al.* explored the use of a CP cathode coated with Pd-P alloy nanoparticles networks (Pd-P NNs) to achieve the selective semihydrogenation of alkynes (Fig. 20) [116]. The systems containing Pd-P NNs displayed higher activity and selectivity for electrocatalytic semihydrogenation of alkynes with H_2O to alkenes with a well-defined configuration than Pd nanoparticles. The incorporation of P could enhance the specific adsorption of alkynes as well as promote the generation of H^*_{ads}, leading to facilitate the hydrogenation of alkynes and suppress the over-hydrogenation. Impressively, this protocol also enabled the synthesis of mono-, di-, tri-deuterated alkenes with the deuterium ratios above 99%. Furthermore, the reaction tolerated various functional groups and achieved a good yield on the gram scale. In the Pd-P||NiSe two-electrode system, 4-vinylaniline and adiponitrile were simultaneously obtained with high yields at the cathode and anode, respectively, which provided a promising prospect for industrial applications.

In a follow up work, they developed a new Cu-S nanowire sponges (NSs) catalyst anchored to the copper foam cathode to promote selective hydrogenation of alkynes to alkenes (Fig. 21) [117]. The experimental and theoretical results indicated that the surface-doped and -adsorbed sulfur on Cu-S NSs played a crucial role in selective alkyne semi-hydrogenation. On the one hand, the formation of sulfur anion-hydrated cation networks facilitated the production of active H* species from electrochemical H_2O splitting. On the other hand, the doping of sulfur decreased the adsorption of alkenes, avoiding over-hydrogenation. In a more recent study, Wang *et al.* employed a carbon-supported Cu microparticles to achieve electrocatalytic semihydrogenation of acetylene with high efficiency and selectivity [118]. By optimizing the Cu-based electrocatalyst to expose more active surfaces, it is conducive to the preferential adsorption and hydrogenation of acetylene, thereby inhibiting hydrogen adsorption and evolution. Combined with modulating the electrode potential to adjust the selectivity of the product, the excessive hydrogenation of acetylene to ethane can be completely avoided at the cathode potential higher than −0.6 V *vs.* RHE.

In addition, Ling *et al.* reported $Ni_{0.85}Se$ nanowires with selenium vacancies ($Ni_{0.85}Se_{1-x}$) *in-situ* grown on NF electrode to promote transfer semihydrogenation of alkynes from H_2O electrolysis (Fig. 22) [119]. The Se vacancy could shift the *d*-band center toward

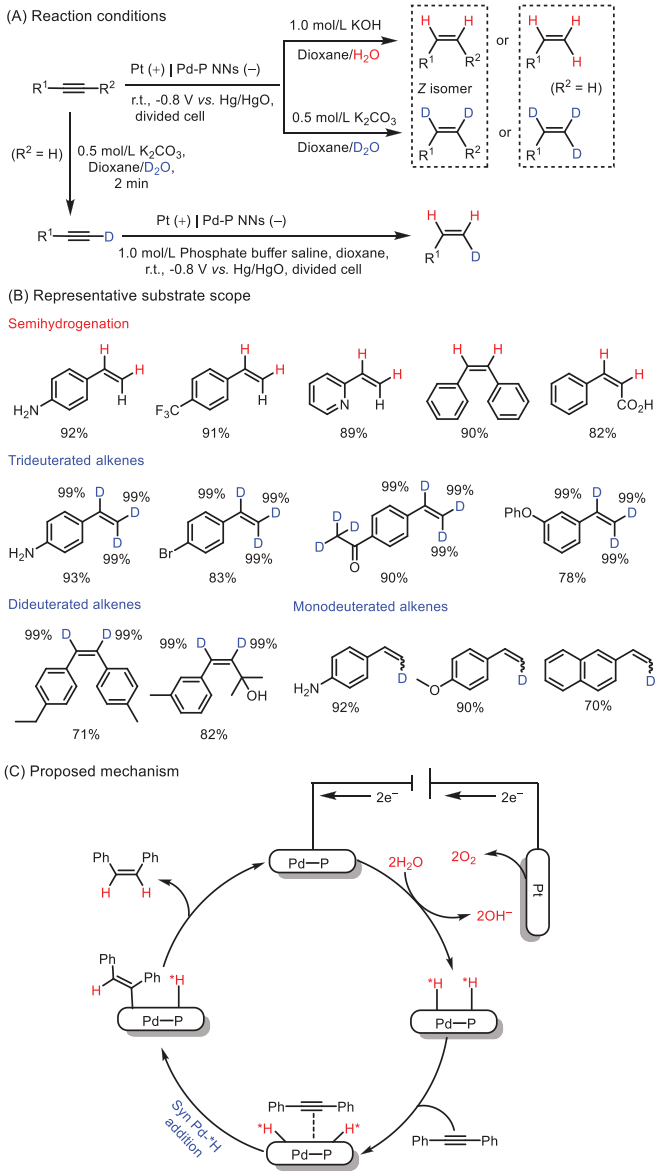

Fig. 20. Pd-P NNs modified electrode for electrocatalytic semihydrogenation of alkynes.

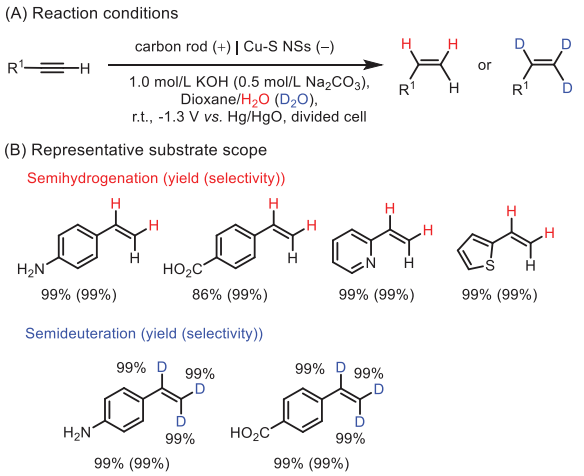

Fig. 21. Cu-S NSs modified electrode for electrocatalytic semihydrogenation of alkynes.

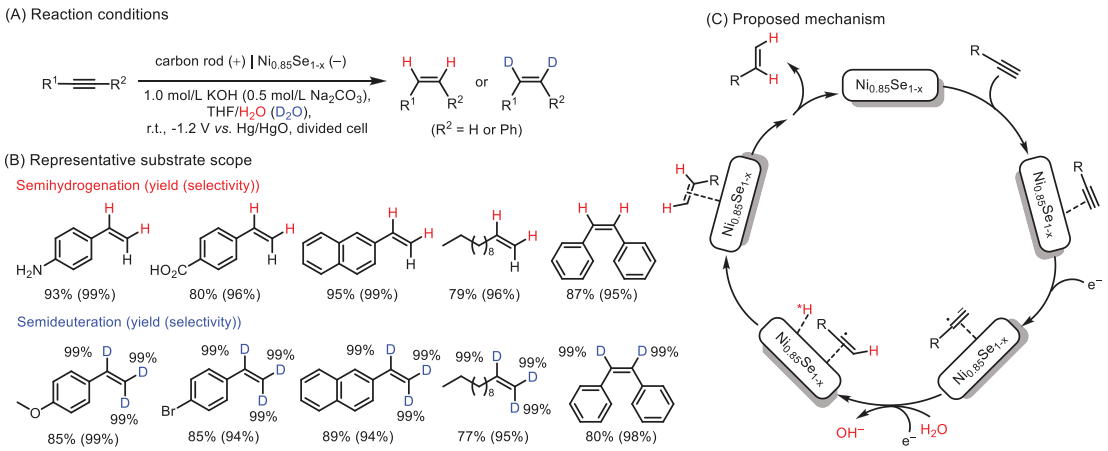

Fig. 22. $Ni_{0.85}Se_{1-x}$ modified electrode for electrocatalytic semihydrogenation of alkynes.

the Fermi level, enhancing the surface adsorption of alkynes and H_2O as well as electron transfer. On the other hand, the Se vacancy could also decrease the activation energy barrier for H_2O dissociation which resulted in facilitating the formation of active H*. And it finally enabled the alkynes conversion up to 99% at a lower potential. Furthermore, 99% alkenes selectivity could be achieved because of the weak adsorption of alkenes as well as the thermodynamic constraints for over-hydrogenation of alkenes to alkanes. In addition, the reaction possessed excellent functional group tolerance and easily obtained deuterated alkenes with the deuterium ratios up to 99% by using D_2O as the deuterated donor.

To sum up, Pd-P, Cu-S and $Ni_{0.85}Se_{1-x}$ modified cathodes enable the efficient construction of alkenes from alkynes under mild conditions and H_2O as the H source. The doping of P, S, and Se could tune the adsorption and desorption of reactants or intermediates with the electrode surface, which will affect the thermodynamics and kinetics of subsequent reaction, and further affect the reaction selectivity. On the other hand, the incorporation of heteroatom might regular the redox capacity of reductants, which will further control the reactivity and selection. In addition, their studies demonstrated that water electrolysis is the rate-determining step, hence, developing more active heterogeneous catalysts to speed up the kinetics of water electrolysis could substantially improve the semi-hydrogenation of alkynes.

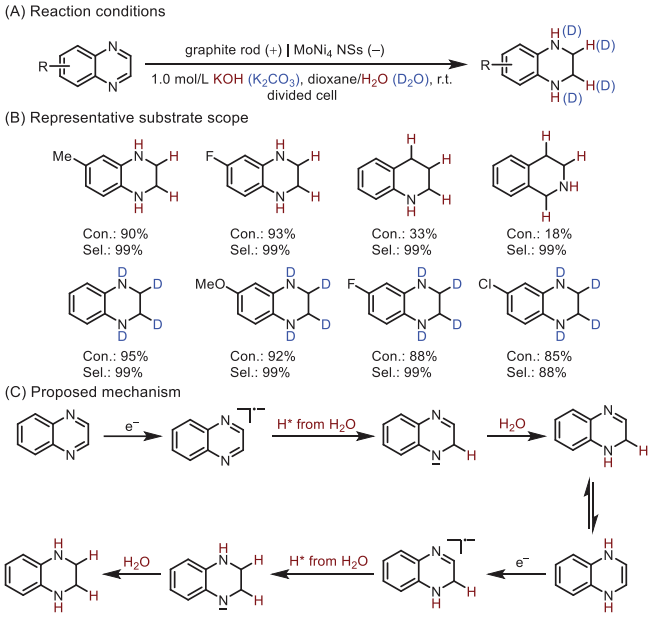

Fig. 23. $MoNi_4$ cathode for electrocatalytic hydrogenation of *N*-heterocycles.

3.2. Electrocatalytic hydrogenation of N-heterocycles

The catalytic hydrogenation of *N*-heteroarenes is of great importance in chemical synthesis, material science, and hydrogen storage transfer. However, it still faces the challenges of breaking the aromaticity of substrates and catalyst poisoning. To date, a number of homogeneous systems based on metal (*e.g.*, Ru, Ir, Pd, and Rh) complexes are active for this kind of transformation [120,121]. Nevertheless, most of them suffer from limited expensive ligands, lack of recyclability, and flammable and explosive H_2 or other expensive/toxic hydrogen sources, hindering their large-scale application. Thus, development of low-cost, safe hydrogen sources, and easily recovered and reused catalysts is urgently demanded. Recently, Li *et al.* exploited 3D self-supported $MoNi_4$ porous nanosheets on NF electrode to achieve electrocatalytic water-involving transfer hydrogenation of *N*-heterocycles (Fig. 23) [122]. A 99% selectivity of 1,2,3,4-tetrahydroquinoxaline and 90% FE were obtained. Electron paramagnetic resonance (EPR) experiment confirmed that the *in-situ* generation of H* from water electrolysis was the key intermediate for quinoxaline hydrogenation *via* radical coupling with the quinoxaline radical anion, and the plausible mechanism was depicted in Fig. 23C. In addition, a variety of *N*-heterocycles hydrogenated products were achieved in moderate to good yields, and easily obtained deuterated products with the deuterium ratios up to 99% by using D_2O as the deuterated donor. Notably, $MoNi_4$ could be used as a bifunctional electrode for electrocatalytic dehydrogenation of *N*-heterocycles, and *in situ* Raman tests revealed that the $Ni^{III}OOH$ formed on the surface of $MoNi_4$ could promote the dehydrogenation process.

3.3. Electrocatalytic hydrogenation of aldehydes/ketones

The selective hydrogenation of carbonyl compounds, especially α,β-unsaturated aldehydes/ketones, is of great significance in industrial production of fine chemicals. Traditional hydrogenation focuses on H_2 as the H source and requires noble metal-based catalysts, which suffer from high cost and safety risk. Hence, it is highly desirable to develop a facile room-temperature hydrogenation method, especially with an inexpensive and safe hydrogen donor. Huang *et al.* employed the $RuO_2-SnO_2-TiO_2/Ti$ as the cathode to achieve highly selective conversion of cinnamaldehyde (CAL) to cinnamyl alcohol (COL) in acidic media (Fig. 24) [123]. The as-prepared $Ru_{0.1}Sn_{0.2}Ti_{0.7}O_2/Ti$ cathode exhibited the highest

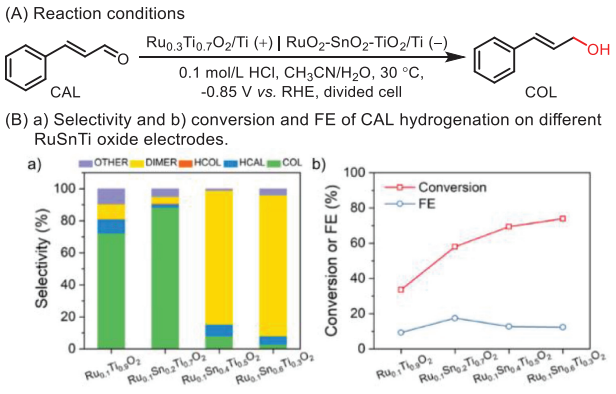

Fig. 24. RuO_2–SnO_2–TiO_2 modified electrode for selective electrocatalytic hydrogenation of CAL. Reproduced with permission [123]. Copyright 2019, American Chemical Society.

COL selectivity with the value of 88.86% at 58.00% conversion of CAL among the reported pure metal and other $Ru_xSn_yTi_{1-x-y}O_2$/Ti electrodes. The experimental and DFT calculation results indicated RuO_2 was the active site, which preferentially interacted with C=O of CAL and decreased the reaction barrier toward COL formation. The doping of SnO_2 could efficiently improve the FE, whereas high SnO_2 content would lead to dimers as the main product. Furthermore, low pH value and high overpotential were also facile to enhance the COL selectivity and inhibit the dimerization product.

Recently, Han *et al.* developed a CP cathode decorated with CoS_2 and CoS_{2-x} nanocapsules (NCs) for the selective hydrogenation of α,β-unsaturated aldehydes (Fig. 25) [124]. Interestingly, CoS_2 NCs and CoS_{2-x} NCs with rich sulfur vacancy exhibited high activity and selectivity for the hydrogenation of CAL to produce hydrocinnamaldehyde (HCAL) and hydrocinnamyl alcohol (HCOL), respectively, which was due to the specific adsorption of the styryl block on CoS_2 and C=O group on the sulfur-defective CoS_{2-x} and the hollow porous structures exposing abundant active sites and improving mass transfer. This work provides an efficient way for the selective hydrogenation of α,β-unsaturated aldehydes and H_2O as the low-cost hydrogen source.

In addition, Chadderdon *et al.* proposed a Ag/C catalyst coated on CP cathode to promote the electrocatalytic hydrogenation of HMF (Fig. 26A) [125]. Though precise control of the cathode potential, the as-prepared Ag/C cathode could highly effective electrocatalytic reduction of HMF to 2,5-bis(hydroxymethyl)furan (BHMF) under mild conditions with 96.2% FE. Unfortunately, the catalytic activity decreased slightly after the first recycle, which was probably due to Ag particle agglomeration. Li *et al.* reported Pd/VN hollow nanospheres coated on CF cathode for electrocatalytic hydrogenation of HMF to 2,5-bishydroxymethyl-tetrahydrofuran (DHMTHF) (Fig. 26B) [37]. The as-obtained Pd/VN/CF cathode exhibited excellent conversion and FE of HMF into DHMTHF with the value of 92% and 91%, respectively. And the values are much higher than those obtained from CF, VN/CF, Pd/C, Pd/V_2O_5/CF and Pd/VOOH/CF electrodes. Furthermore, Pd/VN/CF cathode remained highly active within 8 successive electrolysis processes. Zhang *et al.* reported Cu phosphides nanosheets (Cu_3P) *in situ* grown on carbon fiber cloth (CFC) electrode for electrocatalytic hydrogenation of furfural to furfuryl alcohol (FAL) (Fig. 26C) [81]. The as-obtained Cu_3P/CFC demonstrated excellent catalytic performance with almost 100% selectivity of FAL and above 92% FE, much higher than that of bare CFC, Cu/CFC, Pt/CFC and Ni_2P electrodes. The DFT calculations indicated that the high concentration of H_{ads} was adsorbed on the surface of Cu_3P/CFC and large H_2 desorption energy, facilitating the furfural hydrogenation reaction. In addition, Yang *et al.* demonstrated that copper encapsulated alkaloids composite (alkaloid@Cu) cathode could achieve electrocatalytic asymmetric hydrogenation of aromatic ketones (Fig. 26D) [126]. The alkaloid@Cu directly acted as chiral inducer and could be reused for 10 cycles without obvious reduction of activity.

In another case, Wu *et al.* reported PbS-based materials modified CP electrode for electrochemical reduction of levulinic acid (LA) to γ-valerolactone (GVL) (Fig. 27) [127]. Interestingly, the degree of PbS surface oxidation to $PbSO_4$ significantly affected the catalytic performance, which could be tuned by the calcination temperature. When the PbS was calcined at 400 °C, the prepared PbS-400/CP electrode exhibited the best catalytic performance at a ternary electrolyte consisting of ionic liquids, H_2O and MeCN (FE of 78.6% and current density of 13.5 mA/cm^2) of the electrocatalyst materials reported to date. Moreover, it also showed high selectivity with GVL being the only product. Mechanism studies indicated that LA was transformed into GVL *via* electrochemical hydrogenation followed by subsequent intramolecular esterification.

3.4. Electrocatalytic hydrogenation of nitriles

NH_2 group as a valuable building block in organic synthesis is generally produced by selective hydrogenation of nitriles, which requires high hydrogen pressure and strong alkaline solutions [128]. Compared with thermal hydrogenation, electrocatalytic hydrogenation with H_2O as the proton source to selectively reduce nitriles to the corresponding amines is a promising strategy. In 2021, Zhang *et al.* described a Cu sheet-like nanoarrays *in situ* grown on Cu foil electrode (CuNAs/CuFoil) for electrochemical reduction of aliphatic nitriles to primary amines using H_2O as the H source (Fig. 28) [129]. The as-prepared CuNAs/CuFoil exhibited excellent performance for selective reduction of MeCN to $EtNH_2$ in a CO_2-saturated $KHCO_3$ aqueous solution with a selectivity of 99% and FE of 94%. The experimental and DFT calculations data demonstrated that Cu nanostructure offered preferential adsorption of the nitrile *via* the terminal C≡N group, promoting the hydrogenation process and at the same time suppressing the side reactions, such as HER and CO_2 reduction reaction. Furthermore, the initially formed primary amine can be protected by forming carbamic acids, thus preventing the formation of amine dimers and trimers. Additionally, the reaction tolerated various functional groups and the corresponding primary amines were obtained with exciting selectivity. Recently, Xia *et al.* also proposed a similar idea on MeCN electrohydrogenation in flow reactors [130]. They found that Cu NPs modified cathode exhibited the best $EtNH_2$ FE (~96%) at −0.29 V *vs.* RHE, much higher than Cu microparticles, oxide-derived Cu, and other metals catalysts, such as Ni, Pd, Pt, Sn, In and Bi. The DFT calculations indicated that these results could be attributed to the moderate binding affinity for the reaction intermediates. In addition, the flow reactor could mitigate the anticipated mass-transport limitations as well as led to significantly higher current densities (~1000 mA/cm^2).

3.5. Electrocatalytic reduction of nitroarenes

Selective catalytic hydrogenation of nitroarenes is of great significance for pharmaceuticals, pesticides, and dyestuff in chemical industry [131–136]. As early as 2001, Yuan *et al.* explored Pt/C modified cathode for electrochemical reduction of nitrobenzene [137]. As a result, 57.3% selectivity of cyclohexylanine and 28.2% selectivity of aniline with 8.2% conversion of nitrobenzene were obtained at 70 °C for 2 h. The limitation of the proton transportation as well as the low catalytic activity of the cathodic materials was probably responsible for the lower conversion of nitrobenzene. Hence, developing novel cathodic materials with high conductivity and electrocatalytic activity for the hydrogenation of nitroarene is necessary.

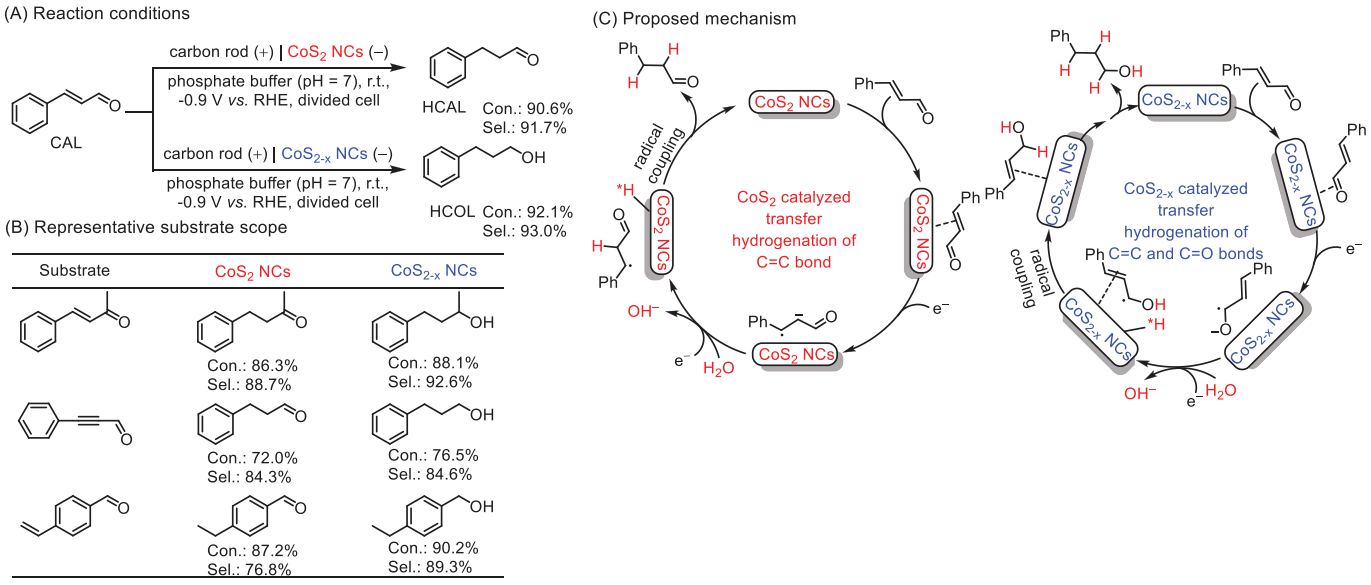

Fig. 25. CoS_2 and CoS_{2-x} NCs modified electrodes for selective electrocatalytic hydrogenation of α,β-unsaturated aldehydes.

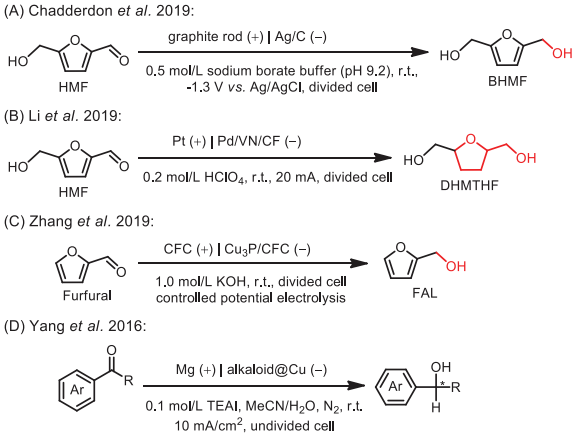

Fig. 26. (A) Ag/C and (B) Pd/VN modified electrodes for electrocatalytic hydrogenation of HMF, (C) Cu_3P/CFC electrode for electrocatalytic hydrogenation of furfural, (D) alkaloid@Cu cathode for electrocatalytic asymmetric hydrogenation of aromatic ketones.

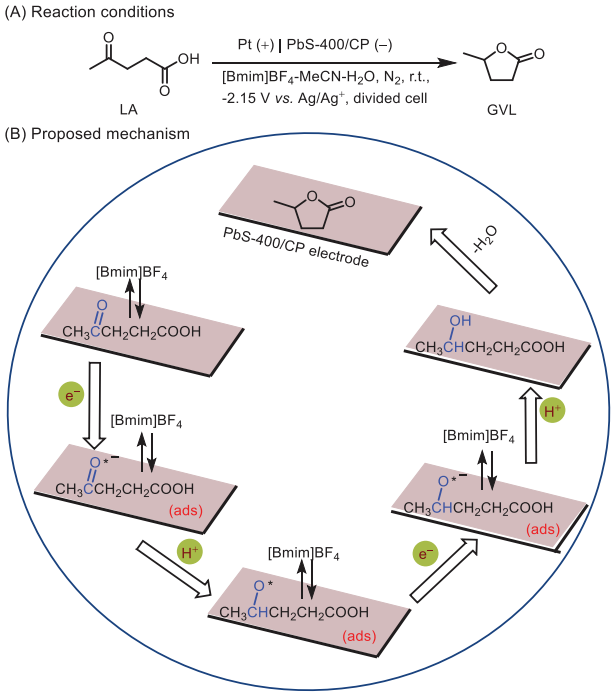

Fig. 27. PbS-400/CP electrode for electrochemical reduction of levulinic acid.

Since then, some bimetal cathodic materials have been prepared and used to enhance the electrocatalytic activity and selectivity for electrochemical reduction of nitrobenzene to aniline [138,139]. For example, Jiang *et al.* reported HF-etched $Cu_{70}Zr_{30}$ amorphous alloy could effective electrocatalytic reduction of nitrobenzene with aniline as the dominant product, which was attributed to the formation and aggregation of Cu nanocrystals on the surface and increased electrochemically active surface area [138]. Additionally, some pure and alloyed Cu-based NPs (Cu-Cu_xO, Pt-Cu alloy and Pt NPs) supported on activated carbon modified cathodes were used for electrocatalytic reduction of nitrobenzene [140–144]. As a pertinent example, Zhang *et al.* investigated the ultrafine Cu_xPt_y alloying nanoparticles anchored on carbon black (donated as Cu_xPt_y/C) employed as a cathode to selectively regulate the products of electrocatalytic hydrogenation of nitrobenzene at different pH and potentials (Fig. 29). The as-obtained Cu_3Pt/C exhibited the best electrocatalytic hydrogenation activity toward nitrobenzene among the prepared Cu_xPt_y/C, owing to the adjusted electronic structure of Cu_3Pt/C could effectively facilitate the adsorption, activation and hydrogenation of nitrobenzene. As a result, the production of aminobenzene was dominant in the acidic media, irrelevant to the applied potential. However, in the alkaline media, azoxybenzene was the dominant hydrogenation product at a low reduction potential of 0.3 V (*vs.* RHE) with 100% conversion and 99% selectivity, while aminobenzene was absolutely dominant at a high reduction potential of −0.3 V (*vs.* RHE) with 100% conversion and 99% selectivity. The theoretical studies indicated that in the alkaline media, the energy barrier of the combination of Ph-NO* with Ph-N* was lower than that of Ph-NH_2*, leading to easily obtained azoxybenzene at low reduction potential and aminobenzene at high reduction potential. As the pH decreased, the free energy of the intermediate decreased, and the reaction would spontaneously obtain aminobenzene.

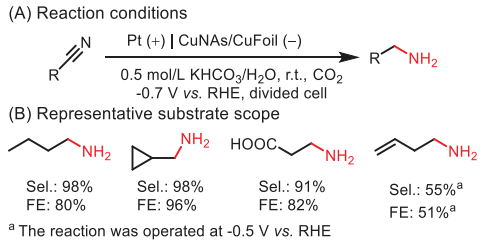

Fig. 28. CuNAs/CuFoil for electrochemical reduction of nitriles.

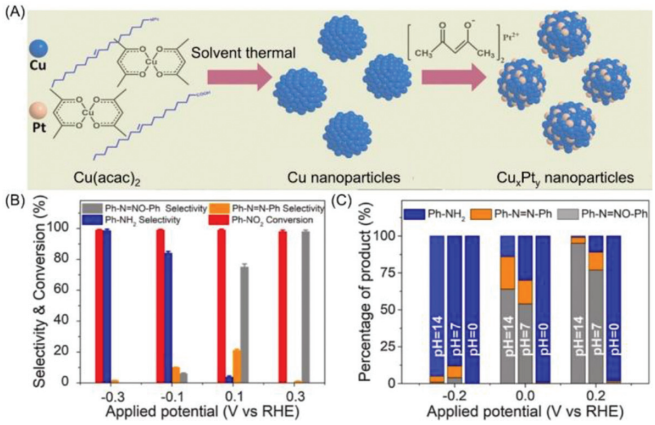

Fig. 29. (A) Schematic illustration of the synthetic process of Cu_xPt_y nanoparticles. (B) The conversion and product selectivity of Ph-NO_2 reduction over Cu_3Pt/C catalyst at different applied potentials. (C) The product selectivity of Ph-NO_2 reduction over Cu_3Pt/C catalyst at different pH solutions and different applied potential. Reproduced with permission [144]. Copyright 2021, Elsevier.

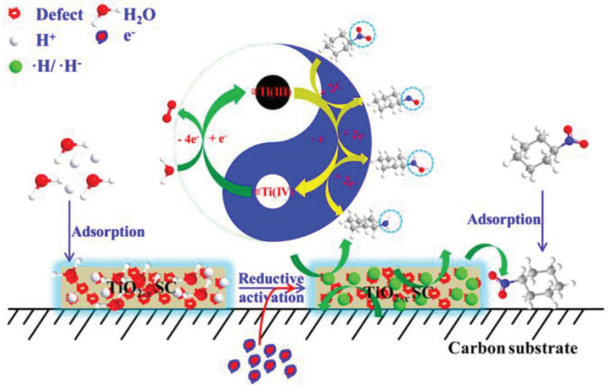

Fig. 30. Defect-centered nitrobenzene reduction mechanism on the defective TiO_{2-x} SCs. (The mixed-valence Ti species cycling between +3 and +4 states at oxygen vacancy sites provide as an efficient electron shuttle and transport route for reductive electrons migrated from carbon cathode to TiO_{2-x} SCs and then to protons to generate active hydrogen (·H/·H⁻). Copied with permission [145]. Copyright 2016, American Chemical Society.

In recent years, several non-noble metallic oxide [145,146], boride [36], phosphide [147], and sulphides [148] have been reported as effective cathodic materials for electrocatalytic reduction of nitro-compounds. For example, Liu *et al.* demonstrated the defect-engineered TiO_{2-x} single crystals (SCs) could be used as an excellent cathodic electrocatalyst for the reduction of nitrobenzene, which was mainly attributed to the defective oxygen vacancy, high-energy [001] facet, as well as the continuous and ordered interior single crystalline structure (Fig. 30) [145].

Recently, Zhang *et al.* reported CoP nanosheet modified NF cathode to promote the selective synthesis of azoxy-, azo- and amino-aromatics by electroreduction of nitro substrates through a potential-tuned strategy (Fig. 31) [147]. A series of desired products bearing various functional groups were obtained with excellent yields and selectivity by applying different bias input. In particular, asymmetrically substituted azoxy-aromatic compounds could also be controllably prepared with moderate to good yields. Additionally, using D_2O instead of H_2O as the sole hydrogen source provided a facile pathway to synthesize deuterated amino-aromatics with high deuterium ratios. Impressively, in a CoP||Ni_2P two-electrode configuration, azoxybenzene and octylnitrile could be simultaneously gram-scale produced with high efficiency at the cathode and anode, respectively. In a subsequent study, they achieved Co_3S_4 ultrathin nanosheets with sulfur vacancies and revealed that sulfur vacancies played a crucial role in the excellent selectivity of nitro hydrogenation, which facilitated the specific adsorption of the nitro group and the intrinsic activity of H_2O electrolysis to form active hydrogen (Fig. 32) [148]. Recently, Huang and Wang *et al.* studied a series of NF-supported spinel oxides MCo_2O_4 (M = Co, Cu, Mn, Fe and Zn) for electrochemical hydrogenation of nitroaromatics, and demonstrated $CuCo_2O_4$/NF was the most effective cathode material owing to the electrogenerated Cu species are the active intermediates [149].

With the development of the electrocatalytic reduction of nitroarenes, inorganic heterogeneous catalysts, as cathodes modifiers

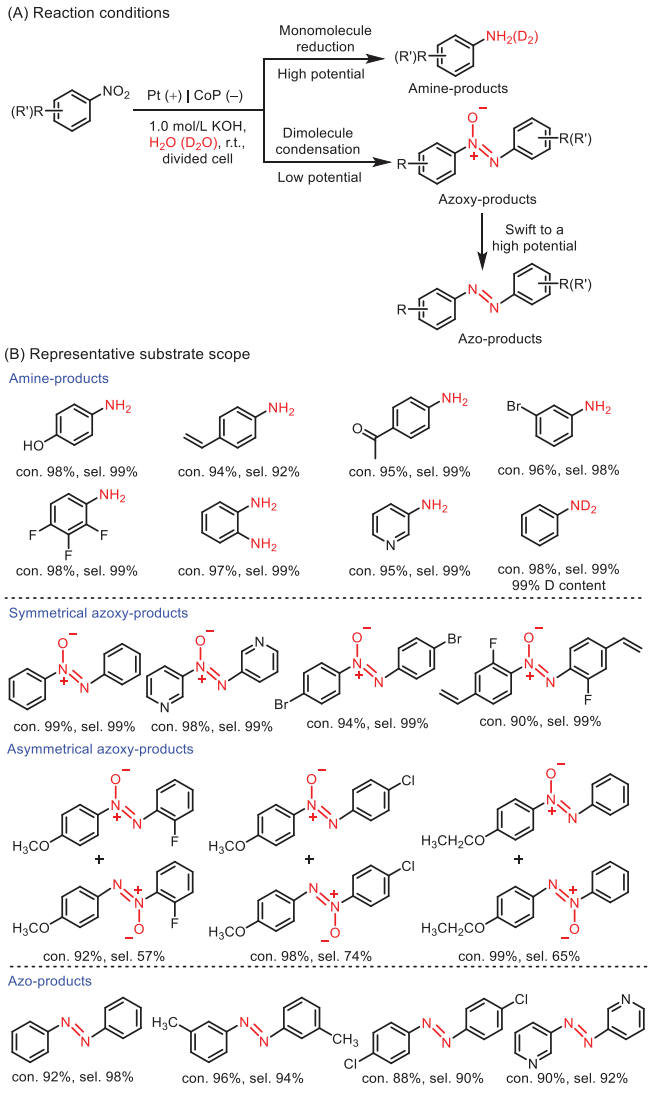

Fig. 31. CoP modified electrode for selective electroreduction of nitro substrates.

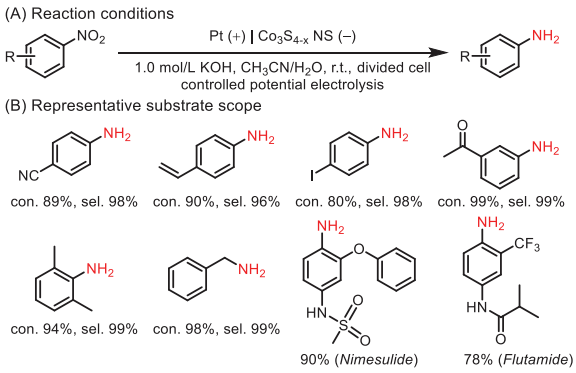

Fig. 32. Co_3S_{4-x} NS modified electrode for electrochemical transfer hydrogenation of nitroarenes.

integrate the advantages of: (1) avoiding the use of strong acid and noble metal cathodes, (2) using H_2O as clean H source, (3) controlling the product by simply tuning the applied voltage. These superiorities may promote heterogeneous catalysts modified electrodes to be widely explored and applied in future.

3.6. Electrocatalytic deuterodehalogenation of halides

The deuterium-labeled molecules are significant for organic mechanism investigation and drug development. The C-H/C-D exchange is a straightforward deuterium incorporation strategy, which commonly required noble-metal catalysts and strong bases/acids. In contrast, the deuterodehalogenation of halides has offered an efficient way to achieve diversified deuterated molecules. However, it usually requires highly active alkyl-metal reagents, noble metal catalysts with complex ligands, and special deuterium donors. At present, electrocatalytic reduction reaction is considered to be an easy method to realize the deuterodehalogenation of halides. For example, Mitsudo *et al.* have achieved electrocatalytic dehalogenative deuteration of aryl halides using 9-fluorenone as an efficient mediator and expensive CD_3CN as D source in an undivided cell equipped with a Zn sacrificial anode and a Pt cathode [150]. Unfortunately, the mechanism was unclear and the yield is moderate. Hence, it is highly desirable to develop novel catalysts to realize highly efficient deuterodehalogenation of halides and elucidate the mechanism.

Recently, Zhang *et al.* proposed a facile electrocatalytic deuterodehalogenation of halides using a self-supported Cu NWAs on Cu foil as the cathode which was fabricated by *in-situ* electrochemical reduction of CuO NWAs (Fig. 33) [151]. The reaction was initiated by the Cu NWAs cathode reduction of halides producing the carbon radical *via* releasing a halogen anion, and the deuterium radicals were simultaneously generated by electrocatalytic D_2O splitting. Then the desired products were formed by radicals cross-coupled reaction. This method possesses the advantages of environmental friendliness, good yields, broad substrate scopes and functional group tolerance. In addition, this electrocatalytic strategy could enable the transformation from C–H to C–D with high yields and deuterium contents *via* a one-pot halogenation-deuterodehalogenation process. Notably, in a Cu NWAs||Ni_2P nanosheets (NSs) two-electrode system, benzen-4-*d*-amine and high-value chemicals such as nitrile, aldehyde, and dihydroquinoline were successfully achieved with excellent yields at the cathode and anode, respectively.

3.7. Electrocatalytic cross-coupling reactions

Allylic alkylation is one of the most important and straightforward tools for C-C bond formation. Traditional methods usually use organometallic reagents to achieve allylic alkylation between an allylic substrate and a carbon nucleophile, which suffers from poor functional-group compatibility, and air/moisture sensitivity [152]. In terms of step economy and practicality, electrochemical allylic alkylations between allylic and alkyl halides is the most promising method. Previous reports demonstrate that electrochemical allylic alkylations need Zn anode to initiate the nucleophilic reaction as well as Pd- and Cu-salts as catalysts [152–154]. Unfortunately, the Pd- and Cu-salts will be reduced to metallic Pd and Cu under the reduction condition, leading to the actual catalytic site is unclear. To address this issue, Yin *et al.* explored CuPd NPs (Fig. 34), Pd NPs and Cu_3Pd NPs modified CP cathodes for the cross-coupling of alkyl halides and allylic halides without using either Zn electrode or Pd-/Cu-salts [155]. Interestingly, the Pd-catalysis was Pd/Cu composition dependent. CuPd NPs exhibited much higher catalytic activity than Pd NPs, indicating Cu played an important role in allylic alkylation. However, Cu_3Pd NPs displayed

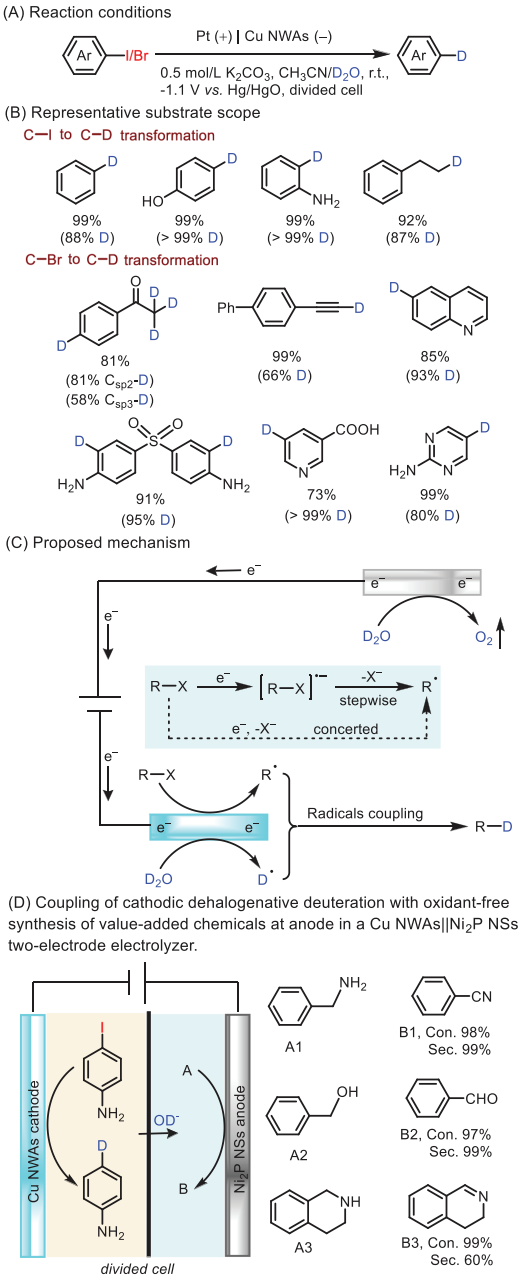

Fig. 33. Cu NWAs modified electrode for radicals coupled reaction.

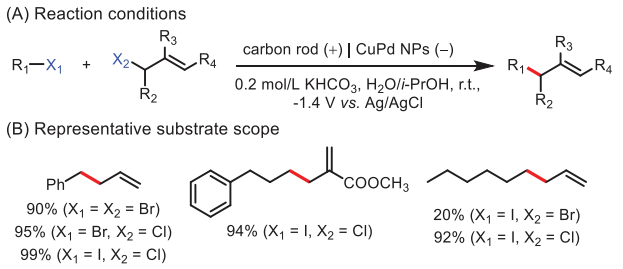

Fig. 34. CuPd NPs modified electrode for electrochemical cross-coupling reaction.

no catalytic activity for this reaction, demonstrating too much Cu would have a negative effect on Pd catalysis. These results illustrated that Pd was the main catalytic sites for C–X activation and Cu as a co-factor to promote the activation *via* binding to halides. And the ratio of Pd/Cu close to 1 is the most efficient catalyst. Moreover, no obvious loss of electrocatalytic activity was observed within five recycles.

4. Summary and perspectives

Organic electrosynthesis, as a "green" technology, has developed rapidly in the past few years. As demonstrated by the above examples, employing heterogeneous catalysts modified electrodes as mediators has opened a new way for innovating organic electrosynthesis. When a suitably modified electrode is used as a heterogenous catalyst, the interaction (adsorption and desorption) of reactants or intermediates with the electrode surface can affect the thermodynamics and kinetics of electron transfer and subsequent reaction, and further affect the selectivity of the whole transformation [156]. The developments highlighted in this review exhibited that heterogeneous electrocatalysts modified electrodes could increase the selectivity and efficiency in organic electrosynthesis. To date, researchers have done lots of work on the development of heterogeneous electrocatalysts modified electrodes in synthetic methodology and designing of novel structures, however, there still present many new challenges and opportunities.

(1) For the design of electrocatalysts: it is well known that the catalytic activity, selectivity, and stability are the main factors to evaluate the performance of electrocatalysts. Firstly, the structure such as 0D quantum dots, 1D nanowires, 2D nanosheets, and 3D framework could significantly affect catalytic activity. However, the structure–performance relationships have not been thoroughly studied. Hence, through precise structure design and fine-tuning the surrounding environment of catalytic sites to adjust the adsorption, chemical bond cleavage and formation, and desorption process is vital important for the catalytic activity and selectivity and urgently needed to explore. Furthermore, some emerging materials could be employed in the organic electrosynthesis. For example, porous framework materials (MOFs and COFs) possess high surface areas, regular arrangement of porous channels and tunable structures and inner environment of cavities, which facilitate the mass transport, electron and charge transfer process, have been applied to the electrocatalytic field [68,70,157–160]. Especially, the preparation of their nanosheets and thin films could increase the accessibility of catalytic sites, thereby improving their catalytic activity [158,161]. However, they have not received much attention in electrocatalytic organic synthesis. We anticipate a bright future for them as promising candidates for electrocatalytic organic synthesis. Secondly, the stability is also a key factor in evaluating the performance of the electrocatalysts. Partial skeleton decomposition of electrocatalysts and the electrocatalysts shedding from electrodes have been found under electrocatalytic conditions (*e.g.*, acidic or alkaline test solution, organic solvents). Therefore, increasing their stability should be also paid close attention.

(2) For the investigation of mechanism: mechanistic studies are crucial for every chemical reaction, and conductive to explore the factors that influence reactivity and selectivity in electrochemical reactions. Therefore, further deciphering the mechanism with the help of the construction of heterogeneous electrocatalysts with precisely controlled and well-defined structure continues to be an important subject, which would be no doubt beneficial for *ab initio* development of heterogeneous electrocatalysts. Recently, a review by Little *et al.* has focused primarily on the analytical techniques that aid in mechanism elucidation in detail, which provide in-depth analysis of ways to understand electroorganic reaction mechanisms [162]. With the rapid development of analysis tools for electrosynthesis, the reaction pathway will be accurately predicted.

(3) For organic electrosynthesis: as mentioned above, heterogeneous catalysts modified electrodes have achieved great improvements in electrocatalytic organic synthesis in recent years. Many common classes of organic reactions are successfully accomplished by heterogeneous catalysts modified electrodes, such as oxidation reaction, reduction reaction, and cross-coupling reactions. However, some fundamental but vital organic reactions, such as the construction of complex chiral centers and the functionalization of inert C(sp^3)–H bonds, are still waiting for exploration. In addition, the synergism of electrochemistry and photochemistry has received much attention, which provides a novel reaction strategy to generate super-oxidants or super-reductants to achieve the difficult molecular transformations under mild conditions [163,164]. Therefore, well-designed electrophotocatalysts to cooperate with electrocatalysis is expected to expand their application in modern organic synthesis.

Water as the nontoxic and low-cost resource has been regarded as a potential oxygen or hydrogen source to replace the traditional oxygenating or hydrogenating agents. However, it faces a big challenge for application due to the high difficulty in activating the O–H bond of H_2O. Recently, some heterogeneous catalysts modified electrodes have been used to split water to offer reactive oxygen or hydrogen in the organic electrosynthesis [36,80,102,116,117,119,124,129,147]. For example, NiB_x and Mn_3O_4 anodes enabled the oxidation of biomass-derived platform chemicals and epoxidation of olefins using H_2O as the oxygen source, respectively [36,102]. Pd-P and CoS_2 cathodes realized the electrocatalytic semi-hydrogenation of alkynes and the selective hydrogenation of α,β-unsaturated aldehydes using H_2O as the hydrogen source, respectively [116,124]. So far, most reports have focused on the conversion efficiency and selectivity of organic reaction, whereas the activation of water, the active sites of electrocatalysts, and the oxygen/hydrogen atom transfer mechanism still remain ambiguous and need to further exploration.

"Paired electrolysis", integrating anodic oxidation reaction with cathodic reduction reaction, enables maximum energy efficiency and the generation of value-added products. To date, the approach of paired electrolysis is mainly focus on the anodic organic oxidation reaction coupled with cathodic hydrogen evolution reaction. Recently, some new paired electrolysis reactions have been reported [115,116,147,151,165]. For example, in a Cu NWAs||Ni_2P nanosheets two-electrode system, benzen-4-*d*-amine and high-value chemicals such as nitrile, aldehyde, and dihydroquinoline were successfully achieved at the cathode and anode, respectively [151]. In a NiSe||NiSe two-electrode electrolyzer, α-nitrotoluenes

and *N*-protected aminoarenes could be simultaneously synthesized with good selectivity and conversion yields [115]. In a CoP||Ni_2P two-electrode configuration, azoxybenzene and octylnitrile could be simultaneously gram-scale produced with high efficiency at the cathode and anode, respectively [147]. In the Pd-P||NiSe two-electrode system, 4-vinylaniline and adiponitrile were simultaneously obtained with high yields at the cathode and anode, respectively [116]. Despite recent advances, paired electrolysis is still very young in the organic electrosynthesis. Balancing the rates of cathodic and anodic reactions is crucial to the reaction efficiency in paired electrolysis. Hence, developing novel electrocatalysts to increase the reaction efficiency and selectivity indicate a new research trend. In addition, the relevant studies still stay in the laboratory stage, developing scalable production method for industrial settings is also urgent.

In a word, integrating heterogeneous electrocatalysts into electrode surfaces expands the range of traditional organic electrosynthesis. Heterogeneous electrocatalysts can be specifically and rationally designed to incorporate catalytic sites and have broad application prospects. Despite there are some difficulties to overcome, heterogeneous electrocatalysts provide a promising platform for advancing electrocatalytic conversions of organic molecules to value-added products.

Declaration of competing interest

The authors declare that they have no known competing financial interests or personal relationships that could have appeared to influence the work reported in this paper.

Acknowledgments

We greatly appreciate the financial support from the National Natural Science Foundation of China (No. 22171154), the Youth Innovative Talents Recruitment and Cultivation Program of Shandong Higher Education, the Natural Science Foundation of Shandong Province (Nos. ZR2020QB114, ZR2020QB008 and ZR2019BB031), Jinan Science & Technology Bureau (No. 2021GXRC080). The project supported by the Foundation (No. ZZ20190312) of State Key Laboratory of Biobased Material and Green Papermaking, Qilu University of Technology (Shandong Academy of Sciences).

References

[1] R. Francke, R.D. Little, Chem. Soc. Rev. 43 (2014) 2492–2521.
[2] E.J. Horn, B.R. Rosen, P.S. Baran, ACS Cent. Sci. 2 (2016) 302–308.
[3] Y. Jiang, K. Xu, C. Zeng, Chem. Rev. 118 (2018) 4485–4540.
[4] P. Xiong, H.C. Xu, Acc. Chem. Res. 52 (2019) 3339–3350.
[5] Y. Yuan, A. Lei, Acc. Chem. Res. 52 (2019) 3309–3324.
[6] L.F.T. Novaes, J. Liu, Y. Shen, et al., Chem. Soc. Rev. 50 (2021) 7941–8002.
[7] Z. Du, Q. Qi, W. Gao, et al., Chem. Rec. 22 (2022) e202100178.
[8] M. Yan, Y. Kawamata, P.S. Baran, Chem. Rev. 117 (2017) 13230–13319.
[9] J. Li, S. Zhang, K. Xu, Chin. Chem. Lett. 32 (2021) 2729–2735.
[10] Q. Tian, J. Zhang, L. Xu, Y. Wei, Mol. Catal. 500 (2021) 111345.
[11] S. Lv, X. Han, J.Y. Wang, et al., Angew. Chem. Int. Ed. 59 (2020) 11583–11590.
[12] L. Ackermann, Acc. Chem. Res. 53 (2020) 84–104.
[13] K.J. Jiao, Y.K. Xing, Q.L. Yang, H. Qiu, T.S. Mei, Acc. Chem. Res. 53 (2020) 300–310.
[14] J. Zhong, Y. Yu, D. Zhang, K. Ye, Chin. Chem. Lett. 32 (2021) 963–972.
[15] J.E. Nutting, M. Rafiee, S.S. Stahl, Chem. Rev. 118 (2018) 4834–4885.
[16] F. Lian, K. Xu, C. Zeng, Chem. Rec. 21 (2021) 2290–2305.
[17] F. Wang, S.S. Stahl, Acc. Chem. Res. 53 (2020) 561–574.
[18] A. Das, S.S. Stahl, Angew. Chem. Int. Ed. 56 (2017) 8892–8897.
[19] L. Yang, L. Cao, R. Huang, et al., ACS Appl. Mater. Interfaces 10 (2018) 36290–36296.
[20] B. You, X. Liu, X. Liu, Y. Sun, ACS Catal. 7 (2017) 4564–4570.
[21] J. Zheng, X. Chen, X. Zhong, et al., Adv. Funct. Mater. 27 (2017) 1704169.
[22] D. Si, B. Xiong, L. Chen, J. Shi, Chem. Catal. 1 (2021) 941–955.
[23] Z. Zhang, K. Deng, ACS Catal. 5 (2015) 6529–6544.
[24] M. Sajid, X. Zhao, D. Liu, Green Chem. 20 (2018) 5427–5453.
[25] H. Luo, J. Barrio, N. Sunny, et al., Adv. Energy Mater. 11 (2021) 2101180.
[26] Y. Zhao, M. Cai, J. Xian, Y. Sun, G. Li, J. Mater. Chem. A 9 (2021) 20164–20183.
[27] G. Grabowski, J. Lewkowski, R. Skowrońsk, Electrochim. Acta 36 (1991) 1995.
[28] D.J. Chadderdon, L. Xin, J. Qi, et al., Green Chem. 16 (2014) 3778–3786.
[29] M. Park, M. Gu, B.S. Kim, ACS Nano 14 (2020) 6812–6822.
[30] N. Jiang, B. You, R. Boonstra, I.M. Terrero Rodriguez, Y. Sun, ACS Energy Lett. 1 (2016) 386–390.
[31] B. You, N. Jiang, X. Liu, Y. Sun, Angew. Chem. Int. Ed. 55 (2016) 9913–9917.
[32] N. Jiang, X. Liu, J. Dong, et al., ChemNanoMat 3 (2017) 491–495.
[33] B. You, X. Liu, N. Jiang, Y. Sun, J. Am. Chem. Soc. 138 (2016) 13639–13646.
[34] S. Barwe, J. Weidner, S. Cychy, et al., Angew. Chem. Int. Ed. 57 (2018) 11460–11464.
[35] J. Weidner, S. Barwe, K. Sliozberg, et al., Beilstein J. Org. Chem. 14 (2018) 1436–1445.
[36] P. Zhang, X. Sheng, X. Chen, et al., Angew. Chem. Int. Ed. 58 (2019) 9155–9159.
[37] S. Li, X. Sun, Z. Yao, et al., Adv. Funct. Mater. 29 (2019) 1904780.
[38] N. Zhang, Y. Zou, L. Tao, et al., Angew. Chem. Int. Ed. 58 (2019) 15895–15903.
[39] L. Gao, Y. Bao, S. Gan, et al., ChemSusChem 11 (2018) 2547–2553.
[40] M.J. Kang, H. Park, J. Jegal, et al., Appl. Catal. B: Environ. 242 (2019) 85–91.
[41] Z. Zhou, C. Chen, M. Gao, B. Xia, J. Zhang, Green Chem. 21 (2019) 6699–6706.
[42] C. Wang, H.J. Bongard, M. Yu, F. Schuth, ChemSusChem 14 (2021) 5199–5206.
[43] X. Huang, J. Song, M. Hua, et al., Green Chem. 22 (2020) 843–849.
[44] S. Choi, M. Balamurugan, K.G. Lee, et al., J. Phys. Chem. Lett. 11 (2020) 2941–2948.
[45] F.J. Holzhäuser, T. Janke, F. Öztas, C. Broicher, R. Palkovits, Adv. Sustain. Syst. 4 (2020) 1900151.
[46] L. Wang, J. Cao, C. Lei, et al., ACS Appl. Mater. Interfaces 11 (2019) 27743–27750.
[47] G. Yang, Y. Jiao, H. Yan, et al., Adv. Mater. 32 (2020) e2000455.
[48] K. Gu, D. Wang, C. Xie, et al., Angew. Chem. Int. Ed. 60 (2021) 20253–20258.
[49] L. Gao, S. Gan, J. Ma, et al., ChemElectroChem 7 (2020) 4251–4258.
[50] L. Gao, Z. Liu, J. Ma, et al., Appl. Catal. B: Environ. 261 (2020) 118235.
[51] S.R. Kubota, K.S. Choi, ChemSusChem 11 (2018) 2138–2145.
[52] M. Sun, Y. Wang, C. Sun, et al., Chin. Chem. Lett. 33 (2022) 385–389.
[53] W.J. Liu, L. Dang, Z. Xu, et al., ACS Catal. 8 (2018) 5533–5541.
[54] M. Zhang, Y. Liu, B. Liu, et al., ACS Catal. 10 (2020) 5179–5189.
[55] H. Chen, J. Wang, Y. Yao, et al., ChemElectroChem 6 (2019) 5797–5801.
[56] B. Zhou, Y. Li, Y. Zou, et al., Angew. Chem. Int. Ed. 60 (2021) 22908–22914.
[57] B.J. Taitt, D.H. Nam, K.S. Choi, ACS Catal. 9 (2019) 660–670.
[58] N. Heidary, N. Kornienko, Chem. Sci. 11 (2020) 1798–1806.
[59] Y. Zhang, Z. Xue, X. Zhao, B. Zhang, T. Mu, Green Chem. 24 (2022) 1721–1731.
[60] B. Zhou, C.L. Dong, Y.C. Huang, et al., J. Energy Chem. 61 (2021) 179–185.
[61] Y. Lu, C.L. Dong, Y.C. Huang, et al., Angew. Chem. Int. Ed. 59 (2020) 19215–19221.
[62] Y. Lu, C.L. Dong, Y.C. Huang, et al., Sci. China Chem. 63 (2020) 980–986.
[63] X. Deng, G.Y. Xu, Y.J. Zhang, et al., Angew. Chem. Int. Ed. 60 (2021) 20535–20542.
[64] O.M. Yaghi, M. O'Keeffe, N.W. Ockwig, et al., Nature 423 (2003) 705–714.
[65] A.P. Cote, A.I. Benin, N.W. Ockwig, et al., Science 310 (2005) 1166–1170.
[66] H.M. El-Kaderi, J.R. Hunt, J.L. Mendoza-Cortes, et al., Science 316 (2007) 268–272.
[67] A. Dhakshinamoorthy, Z. Li, H. Garcia, Chem. Soc. Rev. 47 (2018) 8134–8172.
[68] L. Jiao, Y. Wang, H.L. Jiang, Q. Xu, Adv. Mater. 30 (2018) 1703663.
[69] Y. Wen, J. Zhang, Q. Xu, X.T. Wu, Q.L. Zhu, Coord. Chem. Rev. 376 (2018) 248–276.
[70] X. Zhao, P. Pachfule, A. Thomas, Chem. Soc. Rev. 50 (2021) 6871–6913.
[71] H.Y. Cheng, T. Wang, Adv. Synth. Catal. 363 (2021) 144–193.
[72] L. Ma, S. Wang, X. Feng, B. Wang, Chin. Chem. Lett. 27 (2016) 1383–1394.
[73] L. Hu, C. Dai, L. Chen, et al., Angew. Chem. Int. Ed. 60 (2021) 27324–27329.
[74] S. Yuan, J. Zhang, L. Hu, et al., Angew. Chem. Int. Ed. 60 (2021) 21685–21690.
[75] Y.R. Wang, H.M. Ding, X.Y. Ma, et al., Angew. Chem. Int. Ed. 61 (2022) e202114648.
[76] Y.L. Yang, Y.R. Wang, G.K. Gao, et al., Chin. Chem. Lett. 33 (2022) 1439–1444.
[77] M. Cai, Y. Zhang, Y. Zhao, et al., J. Mater. Chem. A 8 (2020) 20386–20392.
[78] X.J. Bai, W.X. He, X.Y. Lu, Y. Fu, W. Qi, J. Mater. Chem. A 9 (2021) 14270–14275.
[79] M. Cai, S. Ding, B. Gibbons, et al., Chem. Commun. 56 (2020) 14361–14364.
[80] H. Wu, J. Song, H. Liu, et al., Chem. Sci. 10 (2019) 4692–4698.
[81] X. Zhang, M. Han, G. Liu, et al., Appl. Catal. B: Environ. 244 (2019) 899–908.
[82] D. Kaiser, I. Klose, R. Oost, J. Neuhaus, N. Maulide, Chem. Rev. 119 (2019) 8701–8780.
[83] N. Wang, P. Saidhareddy, X. Jiang, Nat. Prod. Rep. 37 (2020) 246–275.
[84] L. Zhang, Y.M. Lee, M. Guo, S. Fukuzumi, W. Nam, J. Am. Chem. Soc. 142 (2020) 19879–19884.
[85] K. Kaczorowska, Z. Kolarska, K. Mitka, P. Kowalski, Tetrahedron 61 (2005) 8315–8327.
[86] S. Liu, B. Chen, Y. Yang, et al., Electrochem. Commun. 109 (2019) 106583.
[87] Y. Liang, S.H. Shi, R. Jin, et al., Nat. Catal. 4 (2021) 116–123.
[88] S. Han, C. Wang, Y. Shi, et al., Cell Rep. Phys. Sci. 2 (2021) 100462.
[89] F.F. Fleming, L. Yao, P.C. Ravikumar, L. Funk, B.C. Shook, J. Med. Chem. 53 (2010) 7902–7917.
[90] R.V. Jagadeesh, H. Junge, M. Beller, Nat. Commun. 5 (2014) 4123.
[91] R.Y. Liu, M. Bae, S.L. Buchwald, J. Am. Chem. Soc. 140 (2018) 1627–1631.
[92] P. Anbarasan, T. Schareina, M. Beller, Chem. Soc. Rev. 40 (2011) 5049–5067.
[93] M.F. Semmelhack, C.R. Schmid, J. Am. Chem. Soc. 105 (1983) 6732–6734.
[94] J. Kim, S.S. Stahl, ACS Catal. 3 (2013) 1652–1656.
[95] K.N. Tseng, A.M. Rizzi, N.K. Szymczak, J. Am. Chem. Soc. 135 (2013) 16352–16355.
[96] Y. Huang, X. Chong, C. Liu, Y. Liang, B. Zhang, Angew. Chem. Int. Ed. 57 (2018) 13163–13166.

[97] I. Mondal, J.N. Hausmann, G. Vijaykumar, et al., Adv. Energy Mater. 12 (2022) 2200269.
[98] S. Torii, K. Uneyama, H. Tanaka, et al., J. Org. Chem. 46 (1981) 3312–3315.
[99] S. Torii, K. Uneyama, M. Ono, H. Tazawa, S. Matsunami, Tetrahedron Lett. 20 (1979) 4661–4662.
[100] K. Rossen, R.P. Volante, P.J. Reider, Tetrahedron Lett. 38 (1997) 777–778.
[101] Y. Zhang, A. Iqbal, J. Zai, et al., Org. Chem. Front. 9 (2022) 436–444.
[102] K. Jin, J.H. Maalouf, N. Lazouski, et al., J. Am. Chem. Soc. 141 (2019) 6413–6418.
[103] K. Kamata, J. Kasai, K. Yamaguchi, N. Mizuno, Org. Lett. 6 (2004) 3577–3580.
[104] C. Gunanathan, D. Milstein, Science 341 (2013) 1229712.
[105] C. Huang, Y. Huang, C. Liu, Y. Yu, B. Zhang, Angew. Chem. Int. Ed. 58 (2019) 12014–12017.
[106] M. Li, C. Liu, B. Zhang, Sci. Bull. 66 (2021) 1047–1049.
[107] Y. Wang, C. Liu, B. Zhang, Y. Yu, Sci. China Mater. 63 (2020) 2530–2538.
[108] L. Yang, F.X. Ma, F. Xu, et al., Chem. Asian J. 14 (2019) 3557–3560.
[109] L. Kesavan, R. Tiruvalam, M.H. Ab Rahim, et al., Science 331 (2011) 195–199.
[110] X. Cao, Z. Chen, R. Lin, et al., Nat. Catal. 1 (2018) 704–710.
[111] B.G. Hashiguchi, S.M. Bischof, M.M. Konnick, R.A. Periana, Acc. Chem. Res. 45 (2012) 885–898.
[112] M. Ravi, M. Ranocchiari, J.A. van Bokhoven, Angew. Chem. Int. Ed. 56 (2017) 16464–16483.
[113] A. Dhakshinamoorthy, A.M. Asiri, H. Garcia, ACS Catal. 9 (2018) 1081–1102.
[114] X. Lin, S.N. Zhang, D. Xu, et al., Nat. Commun. 12 (2021) 3882.
[115] X. Chong, C. Liu, C. Wang, R. Yang, B. Zhang, Angew. Chem. Int. Ed. 60 (2021) 22010–22016.
[116] Y. Wu, C. Liu, C. Wang, S. Lu, B. Zhang, Angew. Chem. Int. Ed. 59 (2020) 21170–21175.
[117] Y. Wu, C. Liu, C. Wang, et al., Nat. Commun. 12 (2021) 3881.
[118] S. Wang, K. Uwakwe, L. Yu, et al., Nat. Commun. 12 (2021) 7072.
[119] Y. Ling, Y. Wu, C. Wang, et al., ACS Catal. 11 (2021) 9471–9478.
[120] R. Yamaguchi, C. Ikeda, Y. Takahashi, K. Fujita, J. Am. Chem. Soc. 131 (2009) 8410–8412.
[121] T. Wang, L.G. Zhuo, Z. Li, et al., J. Am. Chem. Soc. 133 (2011) 9878–9891.
[122] M. Li, C. Liu, Y. Huang, S. Han, B. Zhang, Chin. J. Catal. 42 (2021) 1983–1991.
[123] X. Huang, L. Zhang, C. Li, L. Tan, Z. Wei, ACS Catal. 9 (2019) 11307–11316.
[124] S. Han, Y. Shi, C. Wang, C. Liu, B. Zhang, Cell Rep. Phys. Sci. 2 (2021) 100337.
[125] X.H. Chadderdon, D.J. Chadderdon, T. Pfennig, B.H. Shanks, W. Li, Green Chem. 21 (2019) 6210–6219.
[126] H.P. Yang, Q. Fen, H. Wang, J.X. Lu, Electrochem. Commun. 71 (2016) 38–42.
[127] H. Wu, J. Song, C. Xie, et al., Chem. Sci. 10 (2019) 1754–1759.
[128] D.B. Bagal, B.M. Bhanage, Adv. Synth. Catal. 357 (2015) 883–900.
[129] D. Zhang, J. Chen, Z. Hao, et al., Chem. Catal. 1 (2021) 393–406.
[130] R. Xia, D. Tian, S. Kattel, et al., Nat. Commun. 12 (2021) 1949.
[131] H.U. Blaser, Science 313 (2006) 312–313.
[132] A. Corma, P. Concepcion, P. Serna, Angew. Chem. Int. Ed. 46 (2007) 7266–7269.
[133] A. Corma, P. Serna, P. Concepcion, J.J. Calvino, J. Am. Chem. Soc. 130 (2008) 8748–8753.
[134] J. Song, Z.F. Huang, L. Pan, et al., Appl. Catal. B: Environ. 227 (2018) 386–408.
[135] D. Formenti, F. Ferretti, F.K. Scharnagl, M. Beller, Chem. Rev. 119 (2019) 2611–2680.
[136] T. Wirtanen, E. Rodrigo, S.R. Waldvogel, Adv. Synth. Catal. 362 (2020) 2088–2101.
[137] X.Z. Yuan, Z.F. Ma, Q.Z. Jiang, W.S. Wu, Electrochem. Commun. 3 (2001) 599–602.
[138] J. Jiang, R. Zhai, X. Bao, J. Alloy. Compd. 354 (2003) 248–258.
[139] Z. Chen, Z. Wang, D. Wu, L. Ma, J. Hazard. Mater. 197 (2011) 424–429.
[140] X. Sheng, B. Wouters, T. Breugelmans, et al., ChemElectroChem 1 (2014) 1198–1210.
[141] B. Wouters, X. Sheng, A. Boschin, et al., Electrochim. Acta 111 (2013) 405–410.
[142] X. Sheng, B. Wouters, T. Breugelmans, et al., Appl. Catal. B: Environ. 147 (2014) 330–339.
[143] N. Daems, J. Wouters, C. Van Goethem, et al., Appl. Catal. B: Environ. 226 (2018) 509–522.
[144] M. Jin, Y. Liu, X. Zhang, et al., Appl. Catal. B: Environ. 298 (2021) 120545.
[145] C. Liu, A.Y. Zhang, D.N. Pei, H.Q. Yu, Environ. Sci. Technol. 50 (2016) 5234–5242.
[146] L.Z. Huang, H.C.B. Hansen, M.J. Bjerrum, J. Hazard. Mater. 306 (2016) 175–183.
[147] X. Chong, C. Liu, Y. Huang, C. Huang, B. Zhang, Natl. Sci. Rev. 7 (2020) 285–295.
[148] Y. Zhao, C. Liu, C. Wang, X. Chong, B. Zhang, CCS Chem. 3 (2021) 507–515.
[149] S. Wu, X. Huang, H. Zhang, Z. Wei, M. Wang, ACS Catal. 12 (2022) 58–65.
[150] K. Mitsudo, T. Okada, S. Shimohara, H. Mandai, S. Suga, Electrochemistry 81 (2013) 362–364.
[151] C. Liu, S. Han, M. Li, X. Chong, B. Zhang, Angew. Chem. Int. Ed. 59 (2020) 18527–18531.
[152] Y.L. Lai, J.M. Huang, Org. Lett. 19 (2017) 2022–2025.
[153] J.M. Huang, X.X. Wang, Y. Dong, Angew. Chem. Int. Ed. 50 (2011) 924–927.
[154] J.M. Huang, H.R. Ren, Chem. Commun. 46 (2010) 2286–2288.
[155] Z. Yin, H. Pang, X. Guo, et al., Angew. Chem. Int. Ed. 59 (2020) 15933–15936.
[156] N. Chen, X. Lai, H. Xu, Chin. J. Org. Chem. 40 (2020) 2592–2593.
[157] K. Geng, T. He, R. Liu, et al., Chem. Rev. 120 (2020) 8814–8933.
[158] J. Li, X. Jing, Q. Li, et al., Chem. Soc. Rev. 49 (2020) 3565–3604.
[159] X.F. Lu, B.Y. Xia, S.Q. Zang, X.W.D. Lou, Angew. Chem. Int. Ed. 59 (2020) 4634–4650.
[160] X. Liu, T. Yue, K. Qi, et al., Chin. Chem. Lett. 31 (2020) 2189–2201.
[161] S. Zhao, Y. Wang, J. Dong, et al., Nat. Energy 1 (2016) 16184.
[162] E.C.R. McKenzie, S. Hosseini, A.G.C. Petro, et al., Chem. Rev. 122 (2022) 3292–3335.
[163] J.P. Barham, B. Konig, Angew. Chem. Int. Ed. 59 (2020) 11732–11747.
[164] S. Wu, J. Kaur, T.A. Karl, X. Tian, J.P. Barham, Angew. Chem. Int. Ed. 61 (2022) e202107811.
[165] W. Qiao, I. Waseem, G. Shang, et al., ACS Catal. 11 (2021) 13510–13518.